

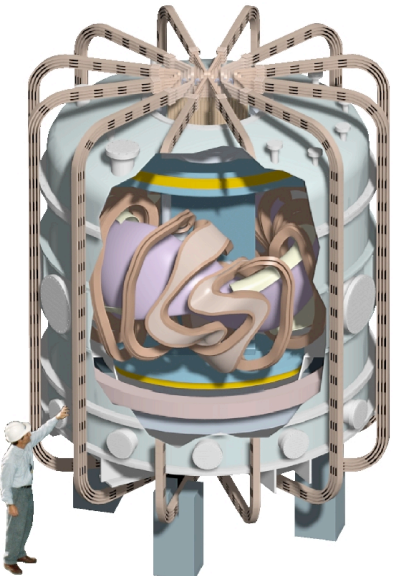
# QPS Transport and Energetic Particle Physics

Don Spong<sup>1</sup>, L. Berry<sup>1</sup>, S. Hirshman<sup>1</sup>, J. Lyon<sup>1</sup>,  
D. Mikkelsen<sup>2</sup>,

<sup>1</sup>Oak Ridge National Laboratory

<sup>2</sup>Princeton Plasma Physics Laboratory

*Sherwood Fusion Theory Conference*  
*April 22 - 24, 2002*  
*Rochester, N. Y.*



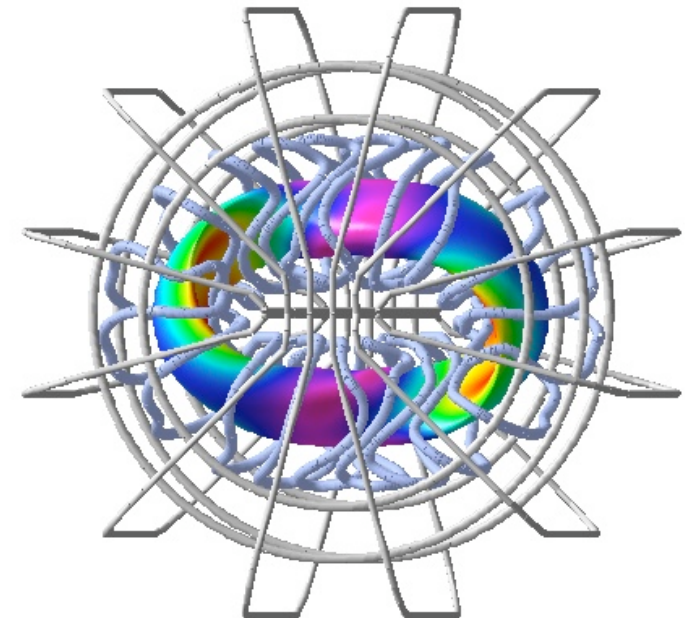
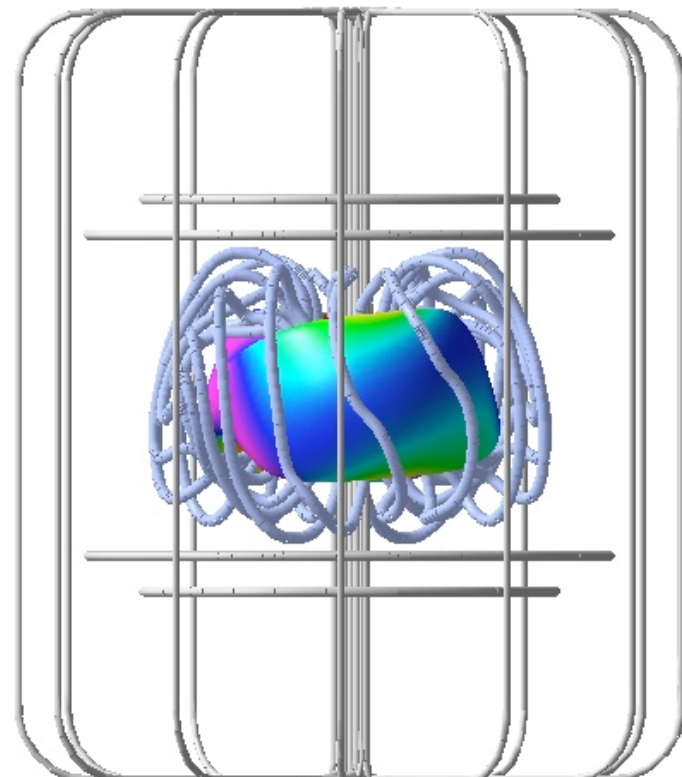
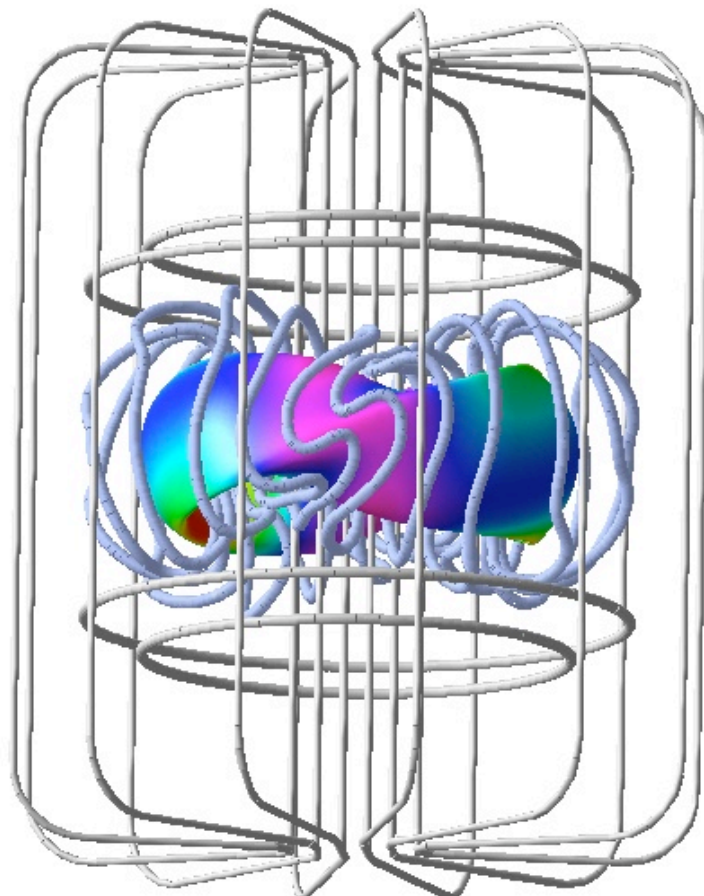
**OAK RIDGE NATIONAL LABORATORY**  
U. S. DEPARTMENT OF ENERGY



# QPS Confinement and Transport Topics

- Is neoclassical stellarator transport sufficiently subdominant to anomalous transport ( $\bar{\eta}_{\text{neo}} \gg \bar{\eta}_{\text{SS95}}$ )?
  - to allow well defined enhanced confinement regimes
  - we consider both low (ECH) and high collisionality (ICH) regimes
- Status of transport tools and QPS predictions
  - simple transport targets used in optimization
  - local diffusive transport models
    - DKES, NEO, 0-D, 1-D calculations
  - global Monte Carlo model
- Bootstrap current levels
  - To what extent do collisional/electric field effects modify bootstrap current?
  - Required incremental Ohmic currents
- Can significant  $\bar{\eta}$ 's be attained?
  - to test bootstrap current/equilibrium robustness
  - to test stability

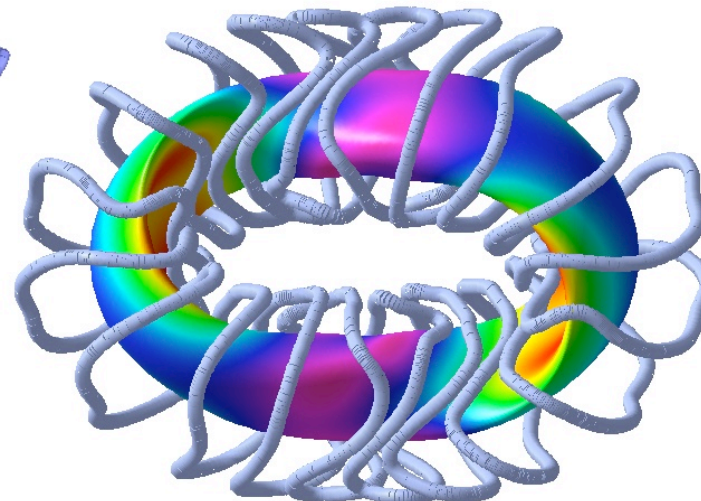
View of recent QPS  
configuration with modular,  
vertical and toroidal field coils:



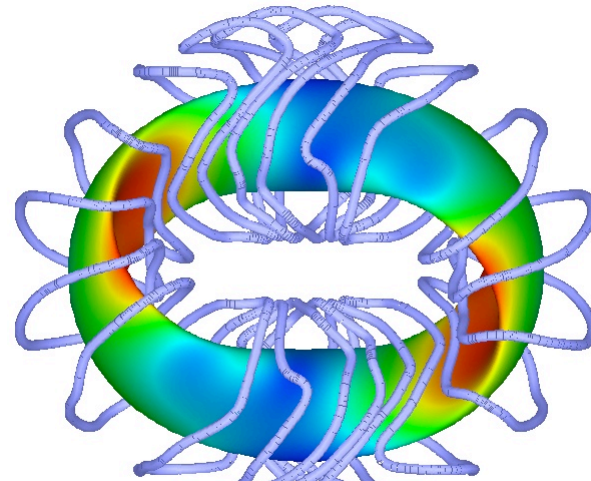
The QPS design has been evolving : several earlier QPS configurations are analyzed here



GB4 - PVR Ref.

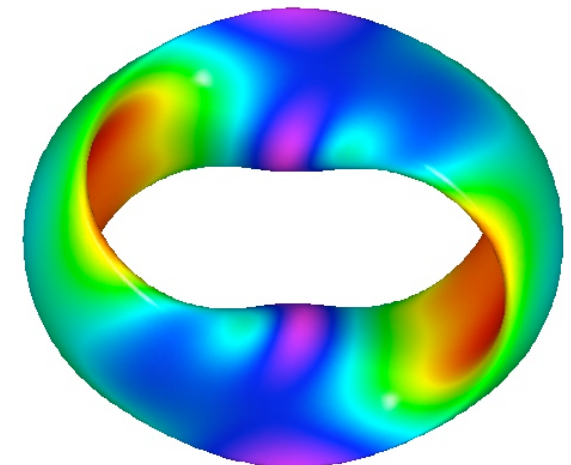


Current  
1108a4

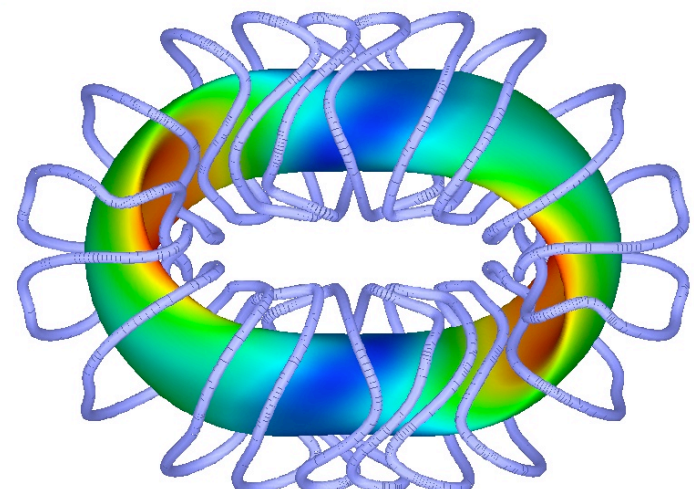


QPS 080301

(similar to 926, 929)



GB5



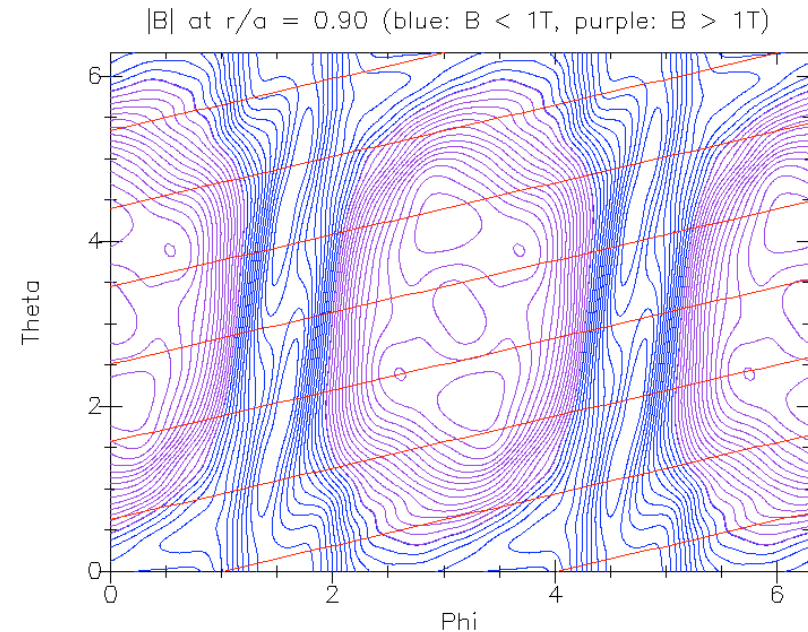
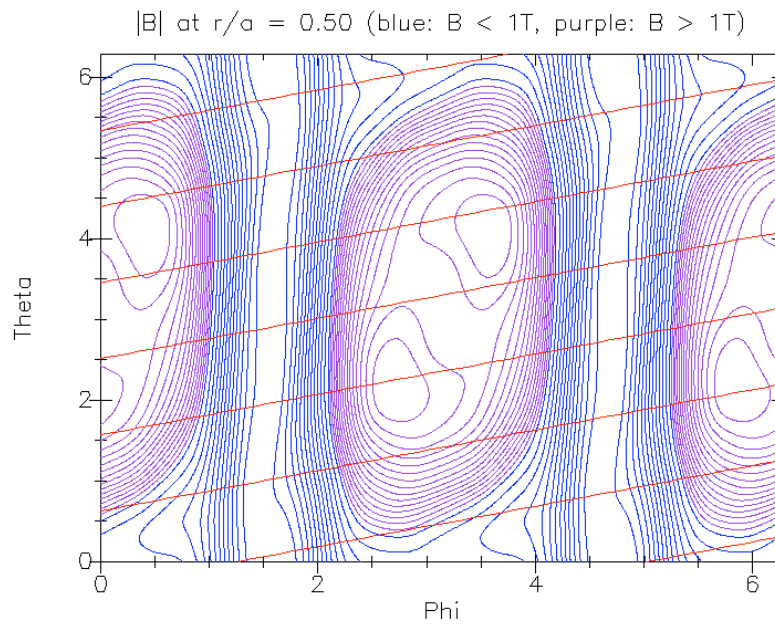
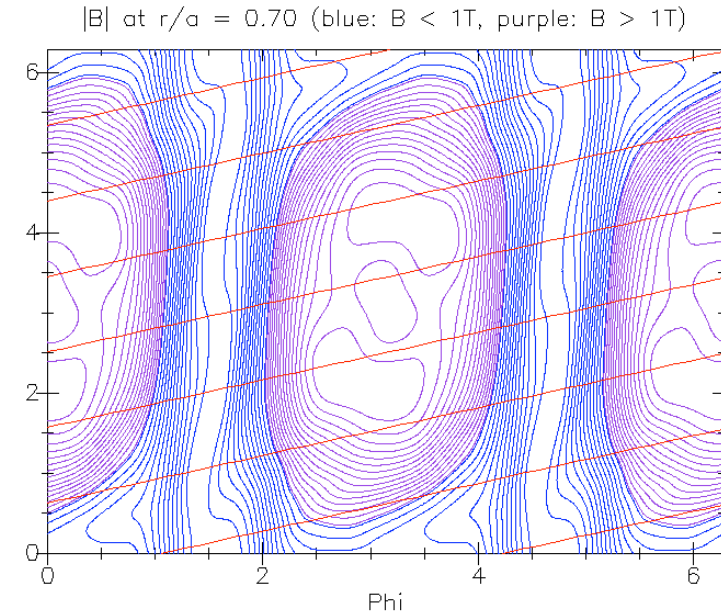
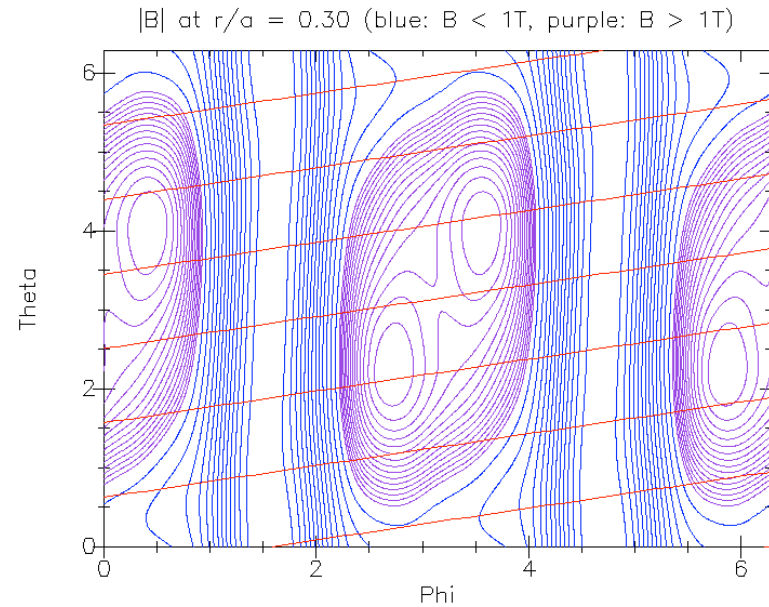
QPS 1016 4

# Transport Tools used to Evaluate QPS configurations:

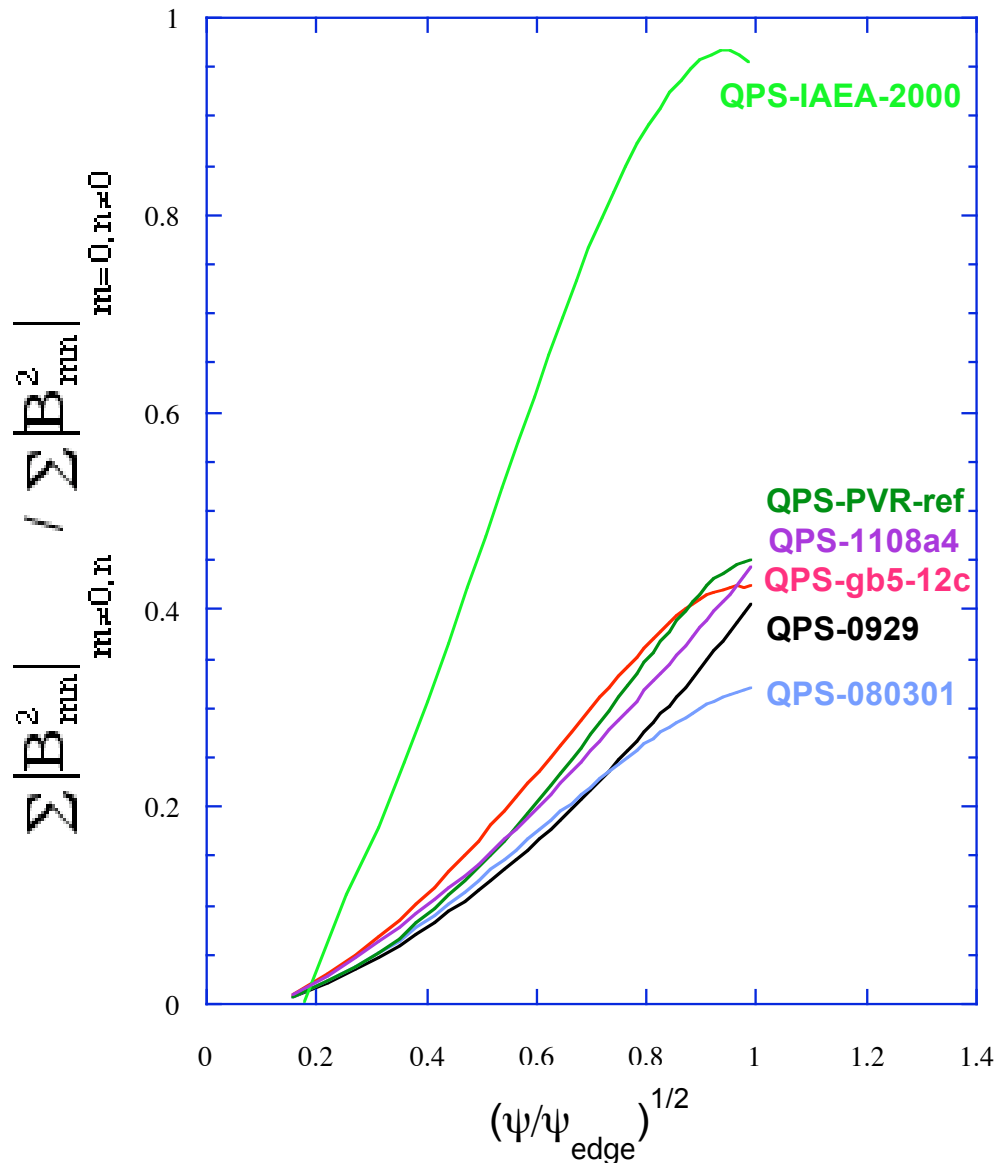
<b>Transport tool</b>	<b>Physical Model</b>	<b>Fixed Parameters</b>	<b>Predicted Parameters</b>
<b>0-D model</b>	ISS95	$P_{heat}$ , $n$	$\bar{Q}$ , $\bar{E}_E$ , $T$
<b>1-D model</b>	ISS95 + Simplified neoclassical	$P_{heat}(r)$ , $n(r)$	$T(r)$ , $\bar{E}_E$ , $P_{loss}(r)$
<b>NEO</b>	$1/\bar{Q}$ , $E_r = 0$ neoclassical	$n'$ , $T'$	$\bar{Q}_{eff}^{3/2}$ Transport coefficient matrix
<b>DKES</b>	Local neoclassical	$n'$ , $T'$ , $E_r$ , $\bar{Q}$	
<b>Monte Carlo</b>	Large orbit global neoclassical	$N(r)$ , $T(r)$ , $\bar{Q}(r)$	$\bar{E}_E$ , $\bar{Q}_b$ , $\bar{Q}_0$

# ***QPS MAGNETIC STRUCTURE***

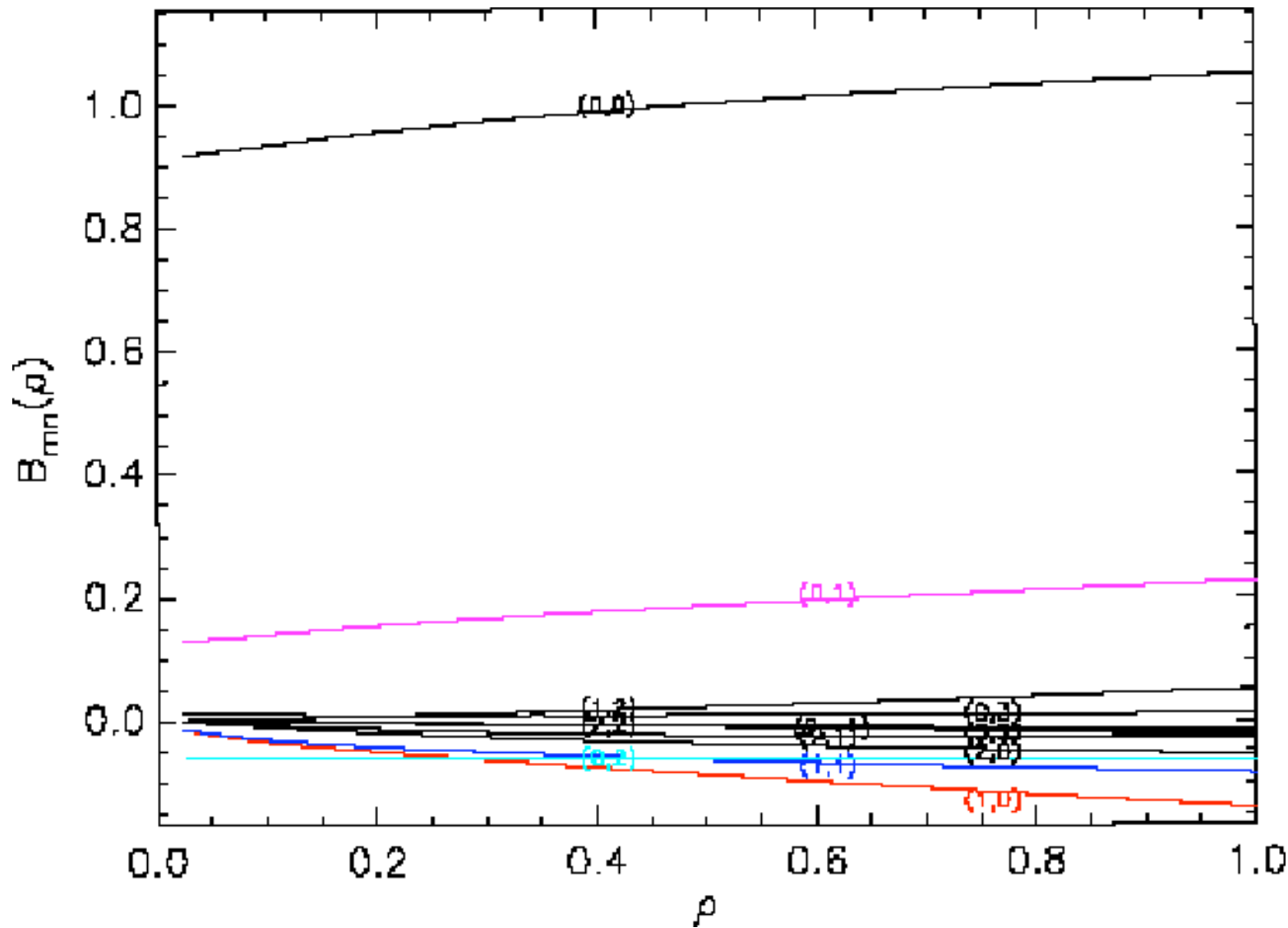
The variation of  $|B|$  on flux surfaces at “ $r/a$ ” = 0.3, 0.5, 0.7, 0.9 shows the quasi-poloidal symmetry about which QPS devices have been optimized:



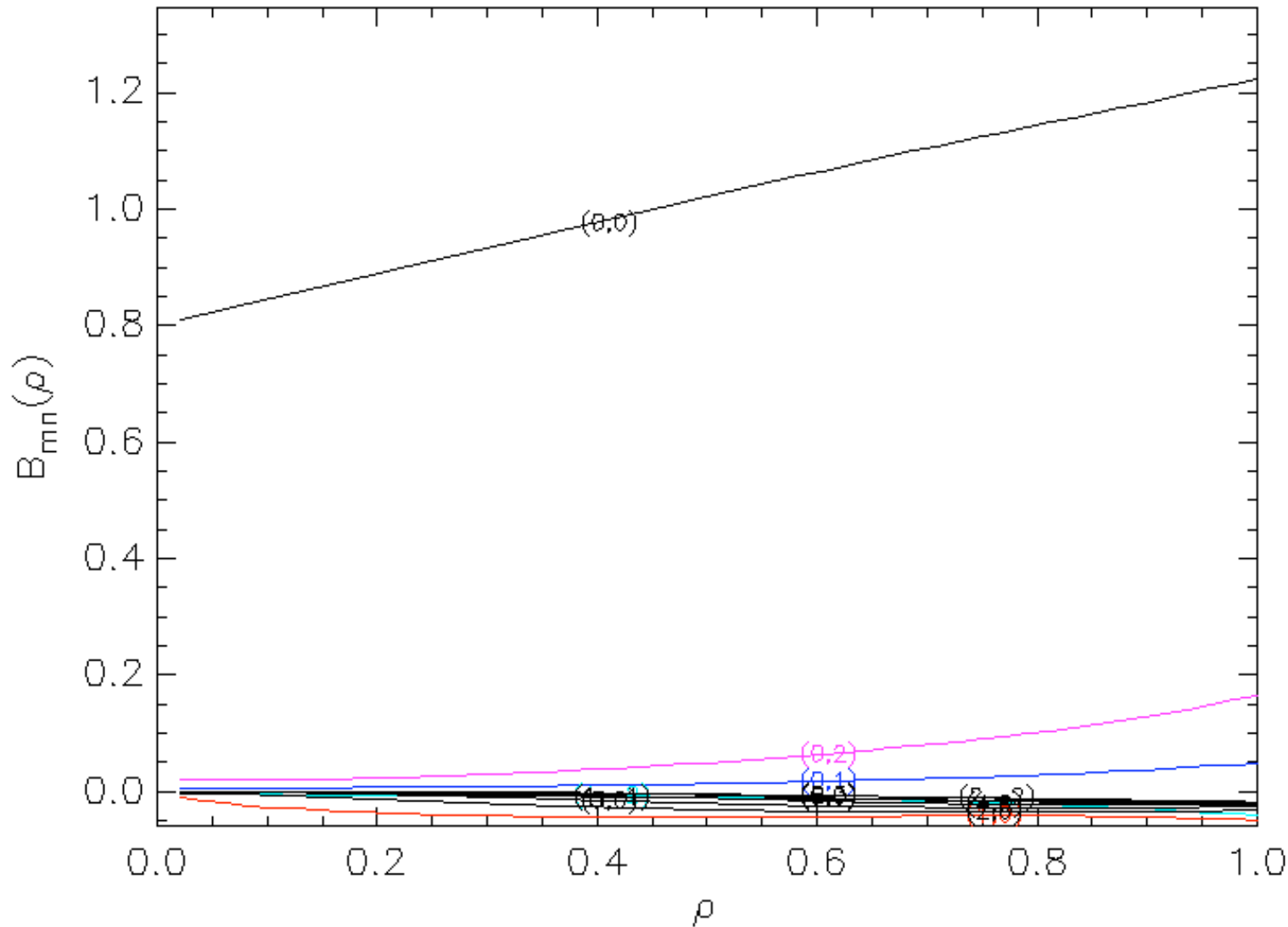
The ratio of magnetic energy in non-poloidally symmetric modes to the magnetic energy in poloidally symmetric modes (excluding  $m = n = 0$ ) is used as a measure of quasi-poloidal symmetry.



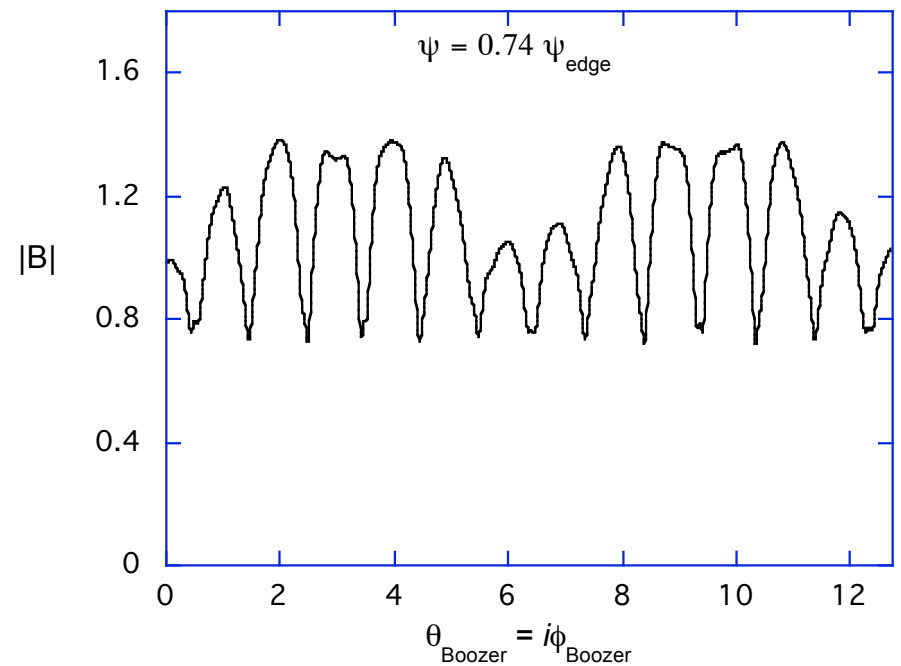
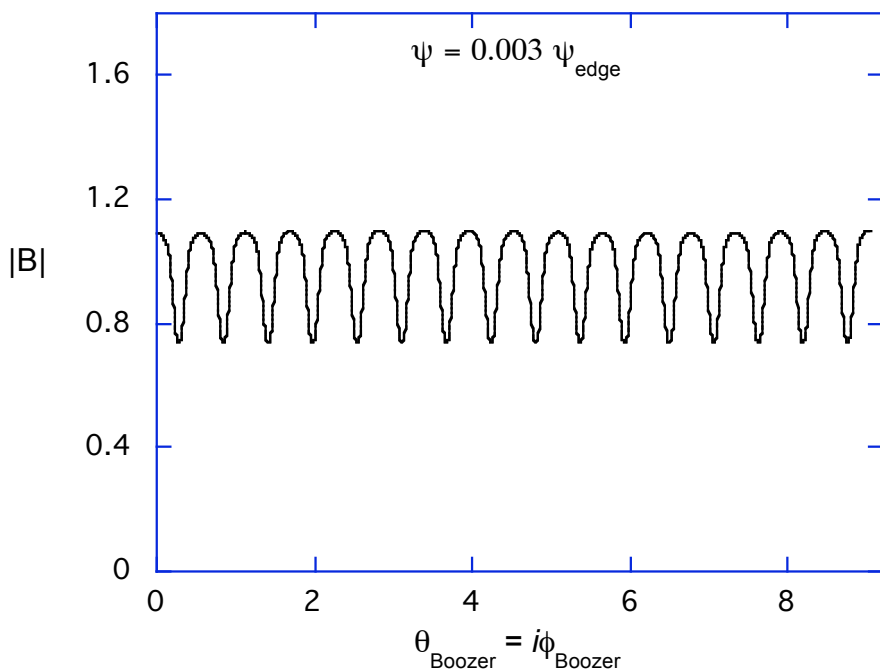
The  $B_{mn}$  spectrum for the QPS 1108a4 device shows that the dominant symmetry is in the poloidal direction



At high  $\beta$ 's (= 15% here) the QPS  $B_{mn}$  spectrum becomes increasingly quasi-poloidal.



Variation of  $|B|$  along a field line for QPS\_1016 configuration (near axis and edge): Minima are well aligned leading to good trapped particle confinement



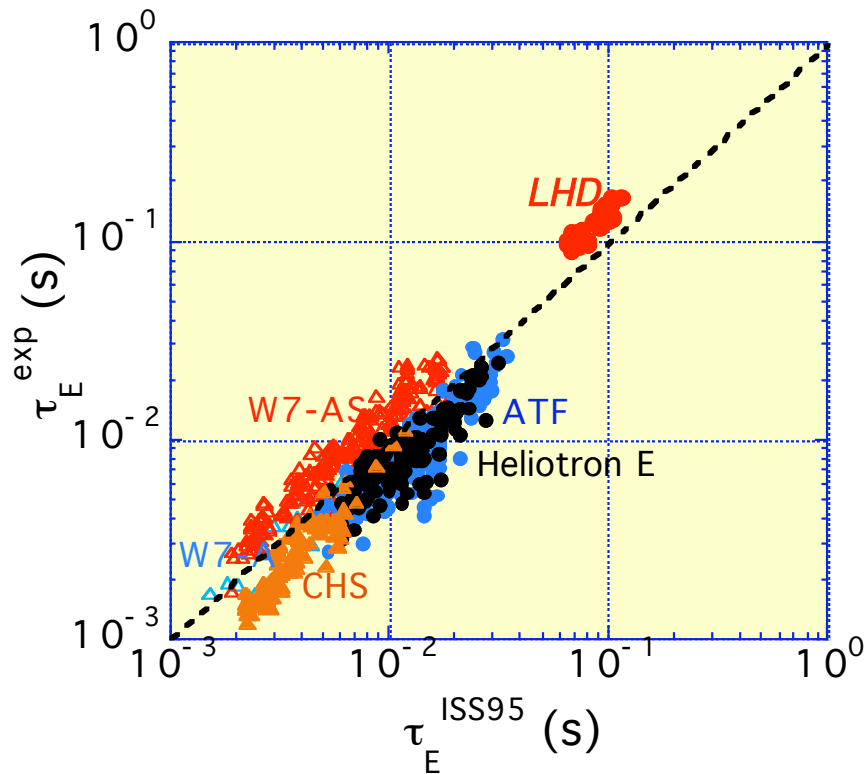
# ***QPS O-D AND 1-D TRANSPORT ANALYSIS***

# Global stellarator confinement scalings

$$\bar{\square}_E^{\text{ISS95}} = 0.079 H_{\text{ISS95}} a_p^{2.21} R^{0.65} P^{-0.59} n^{0.51} B^{0.83} \bar{\square}^{0.4}$$

$$\bar{\square}_E^{\text{ISS95}} = W_{\text{tot}} / P \quad W_{\text{tot}} = 1.5 \langle \bar{\square} \rangle (\bar{\square}_0^2 / 2 \bar{\square}_0) V_p \quad \text{0-D model}$$

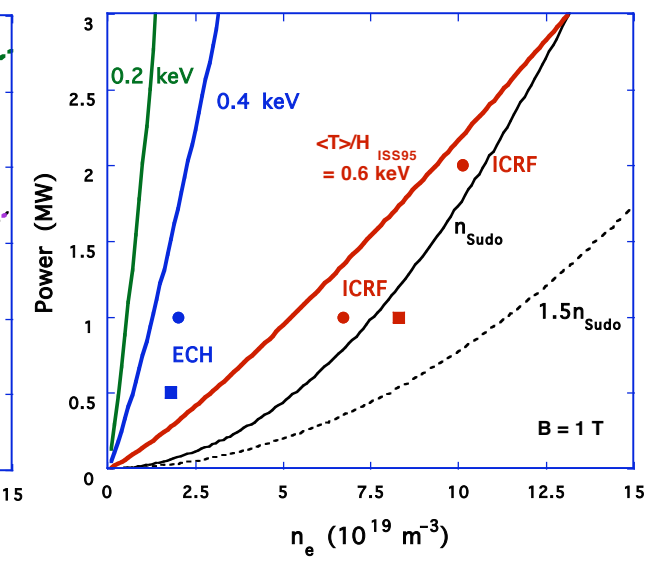
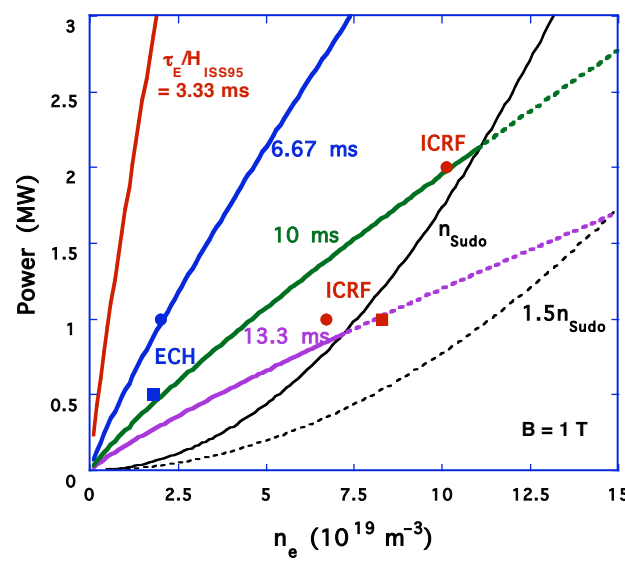
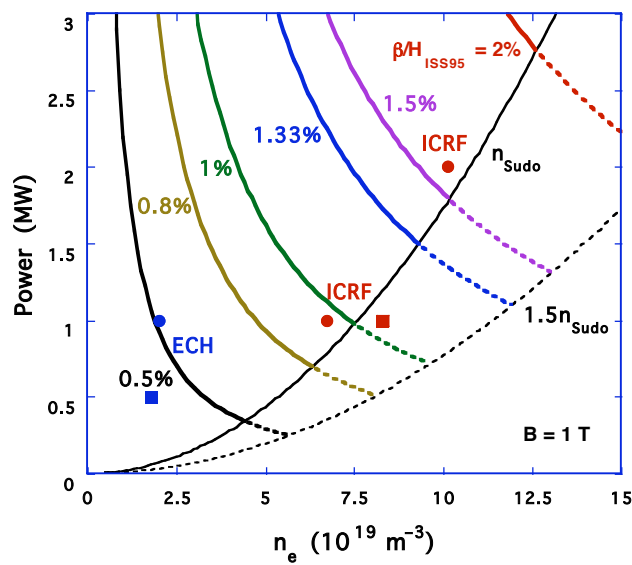
$$n_{\text{Sudo}} = 0.25 [P B / R a_p^2]^{1/2}$$



- Data only for  $R/a_p > 5$
- W7-AS and LHD find  $H_{\text{ISS95}}$  up to 2.5
  - low shear, large  $a_p$
- For fixed  $a_p, R, n, B, \bar{\square}$  can calculate:
  - $\langle T \rangle / H_{\text{ISS95}}$
  - $\langle \bar{\square} \rangle / H_{\text{ISS95}}$
  - $\bar{\square}_E / H_{\text{ISS95}}$

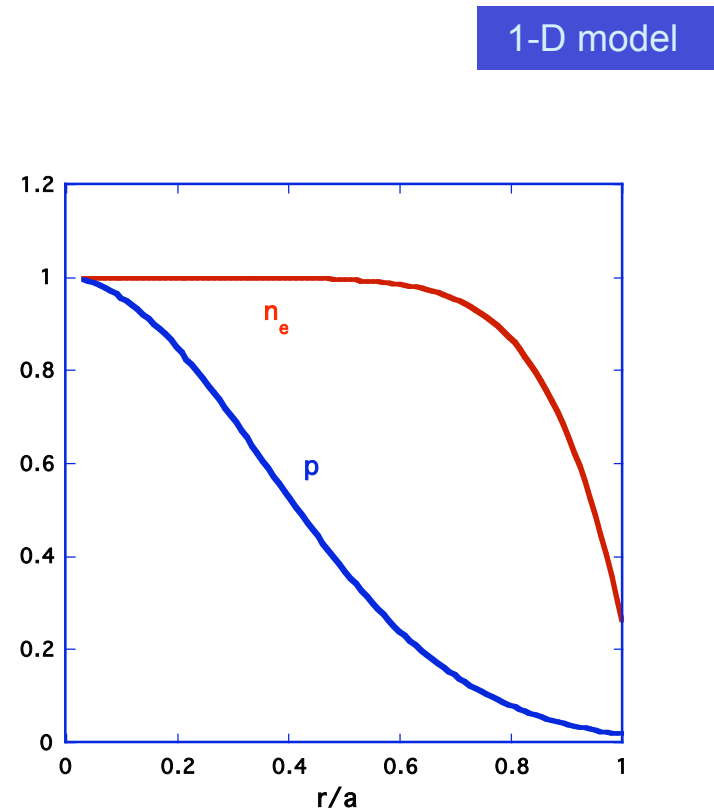
# Global stellarator confinement scalings indicate the QPS CE device can achieve adequate plasma performance for its mission

0-D model



# 1-D Model (Dave Mikkelsen) includes profile effects and self-consistent ambipolar electric field

- Coupled electrons/ion power balance equations
- Ambipolar particle balance for helical ripple component
- Thermal diffusivities
  - Neoclassical ripple coefficient using  $\Box_{\text{eff}}^{3/2}$  from NEO code
  - $E_r$  dependence from Shaing-Houlberg single helicity model
- Density and power deposition profiles assumed as shown

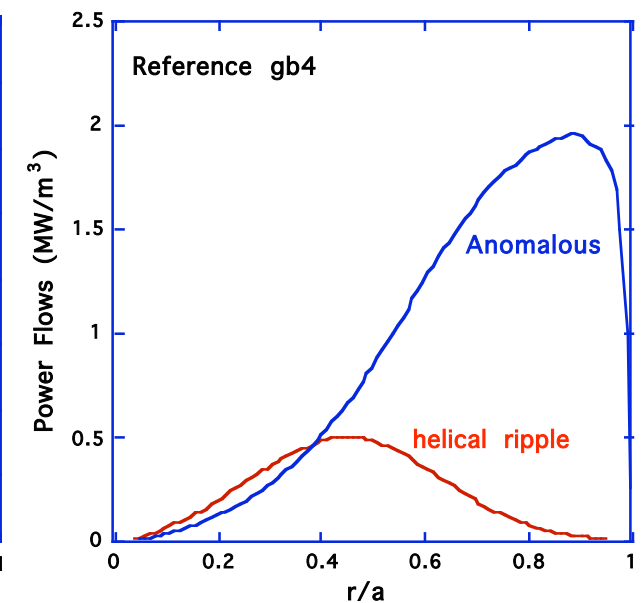
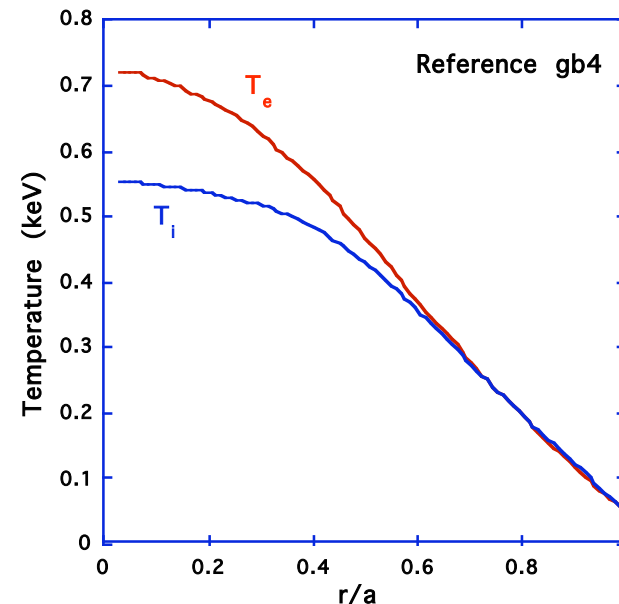
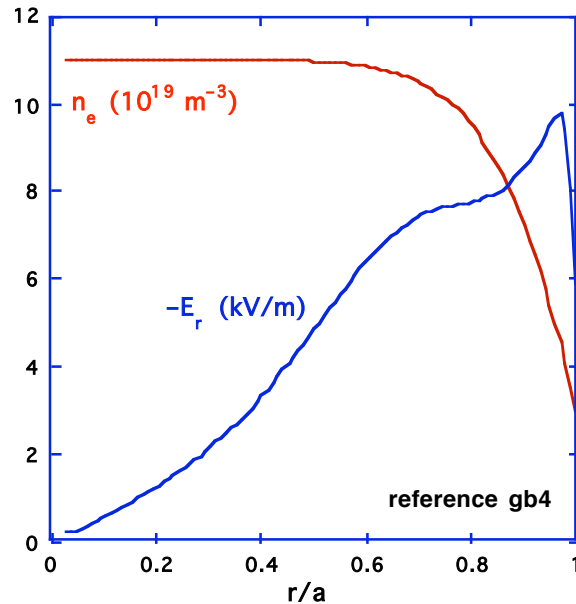


This model has been motivated by more comprehensive calculations (DKES, Monte Carlo)

# ICRF Heated plasmas

Device	$\Delta t$ (msec)	$\langle \Delta \rangle$	1-D model
gb4	18.3	1.4	
gb5_12c	18.8	1.44	
gb5_12d	18.9	1.46	

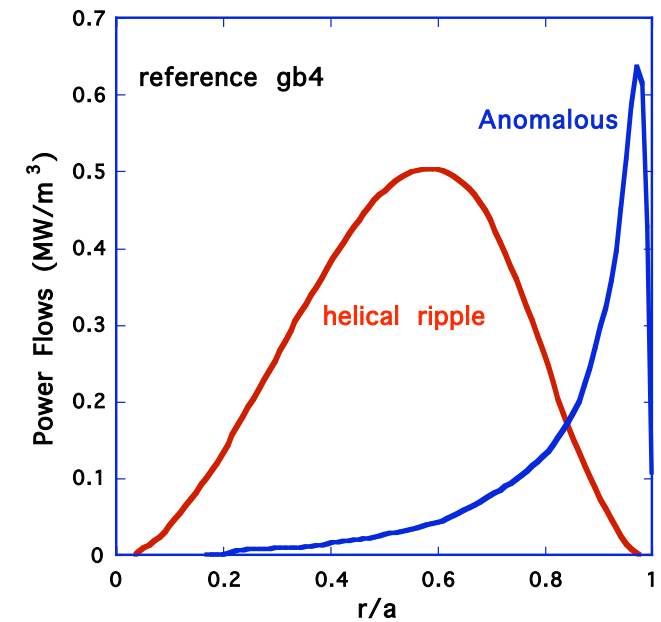
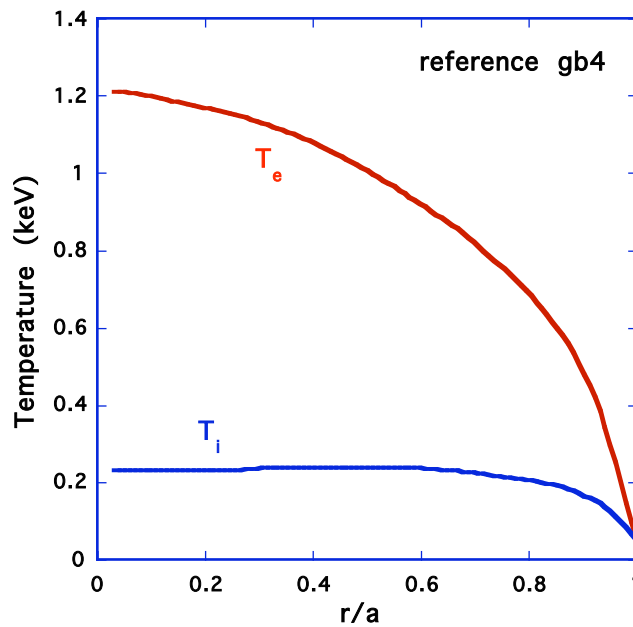
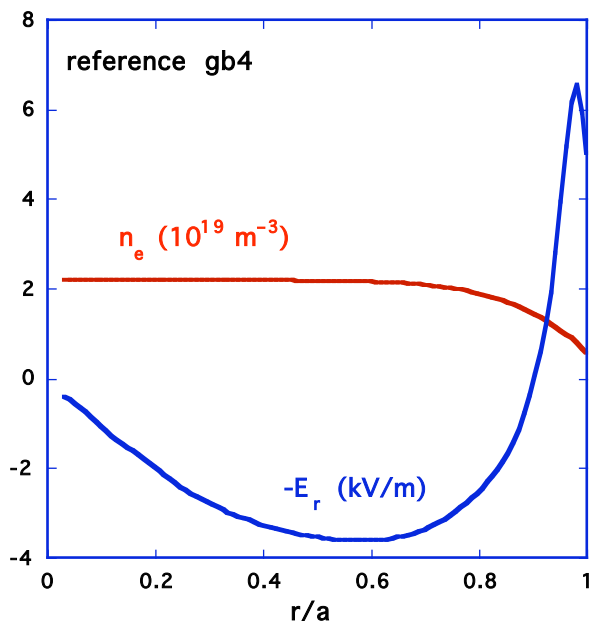
For  $B = 1\text{T}$ ,  $P_{\text{ICRF}} = 1\text{Mw}$



# ECRF Heated plasmas - gb4 configuration

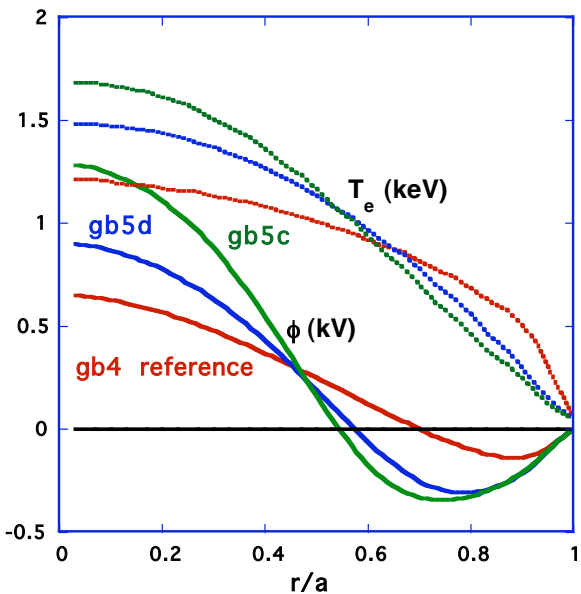
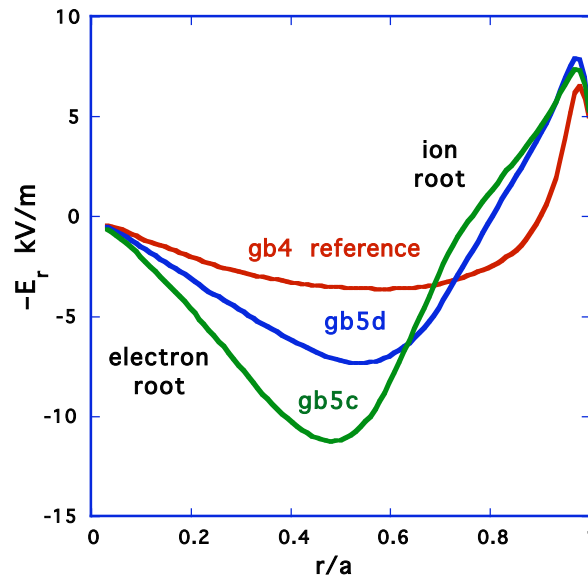
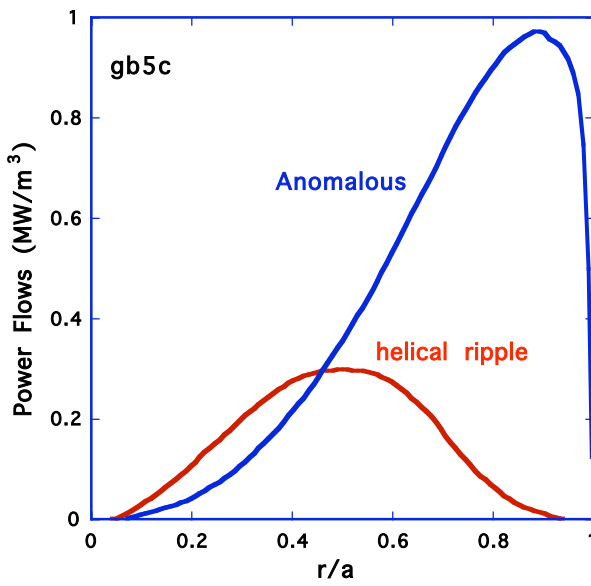
Device	$\bar{\tau}_E$ (msec)	$\langle \bar{\tau} \rangle$	1-D model
gb4	10.0	0.77	

For  $B = 1\text{T}$ ,  $P_{\text{ECRF}} = 1\text{Mw}$



# ECRF Heated gb5 configuration has helical ripple component that is subdominant to anomalous

Device	$\Delta E$ (msec)	$\Delta E$	1-D model
gb4	10.0	0.77	
gb5c	10.1	0.78	
gb5d	10.2	0.79	



# ***QPS DKES AND NEO TRANSPORT ANALYSIS***

# The DKES (Drift Kinetic Equation Solver) provides the full neoclassical transport coefficient matrix (multi-helicity)

DKES Transport analysis

$$I_i = \frac{1}{T} \vec{Q} \cdot \vec{s} + n \langle (\vec{u} \cdot \vec{u}_s) \cdot \vec{B} \rangle$$

$$A_j = \sum_{j=1}^3 \hat{D}_{ij} A_j$$

$$\hat{D}_{ij} = n \frac{2}{\sqrt{\pi}} \int_0^\infty dK \sqrt{K} e^{iK} g_i g_j D_{ij}$$

where  $g_1 = g_3 = 1, g_2 = K, K = \frac{v}{V_{th}}$

$$D_{11} = D_{12} = D_{21} = D_{22} = \frac{V_{th}}{2} \frac{\partial v_{th}}{\partial r} \frac{\partial}{\partial r} L_{11}$$

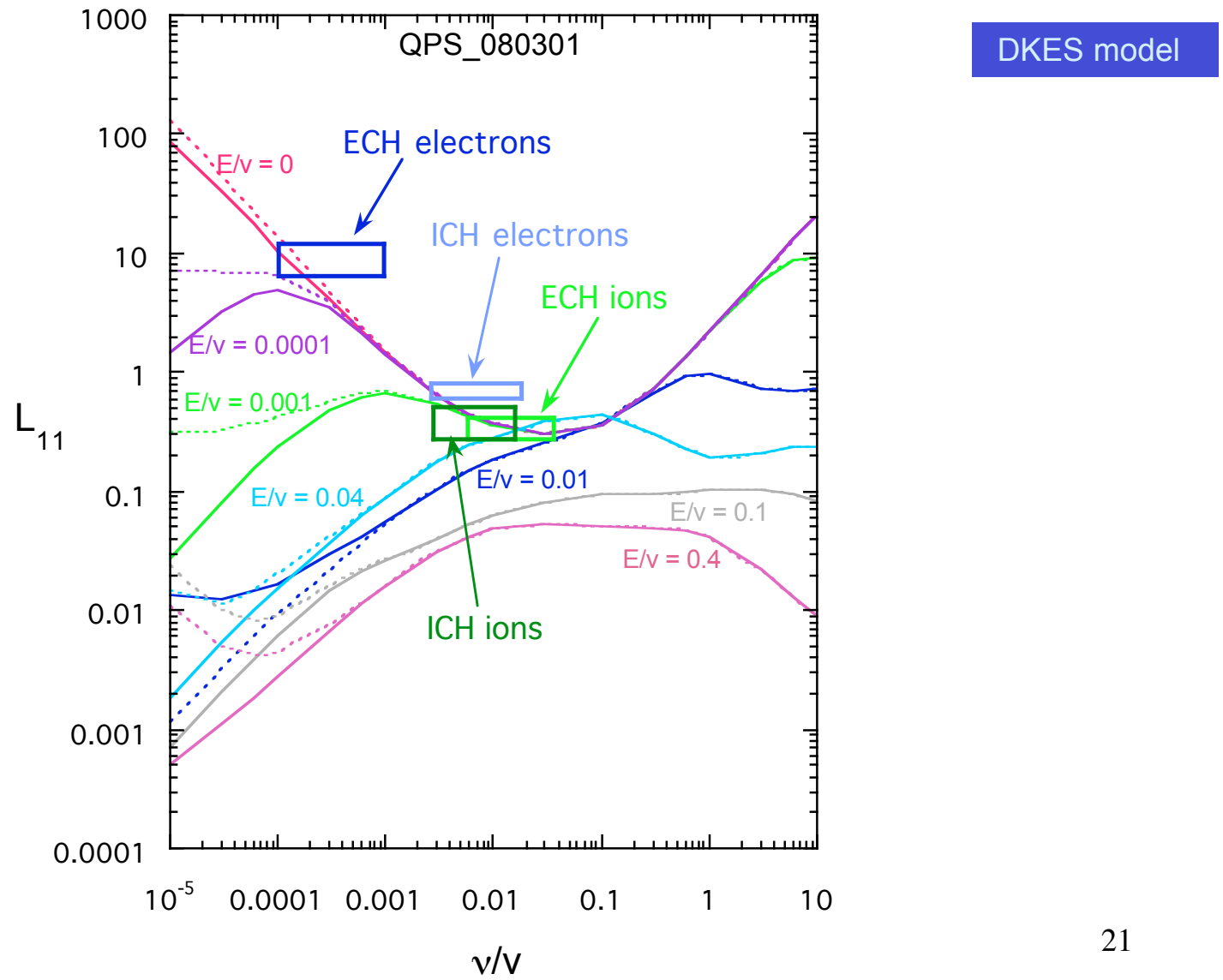
$$D_{31} = D_{32} = D_{13} = D_{23} = \frac{V_{th}}{2} \frac{\partial v_{th}}{\partial r} \frac{\partial}{\partial r} L_{31}$$

$$D_{33} = \frac{V_{th}}{2} \sqrt{K} L_{33}$$

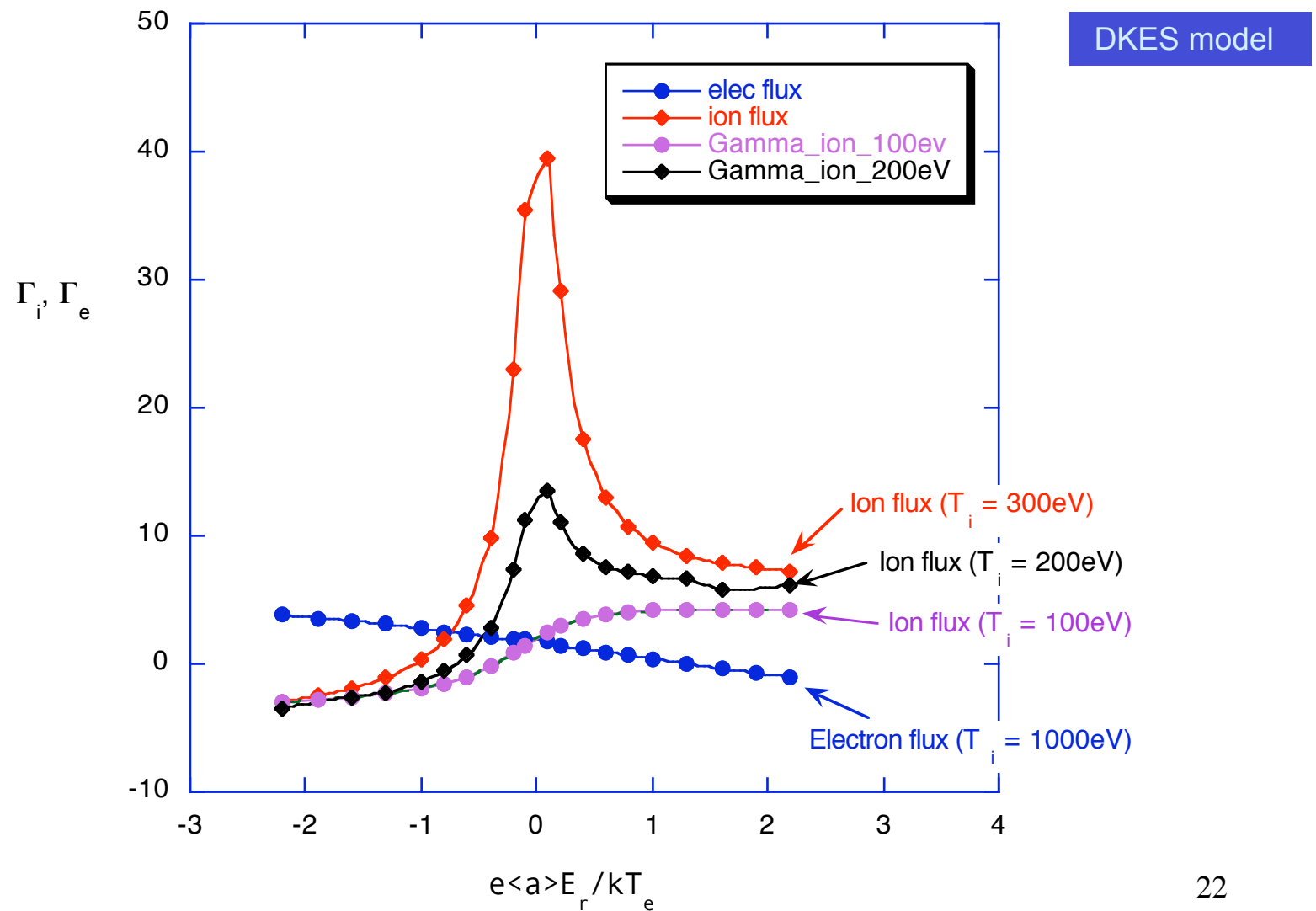
$$L_{ij} = L_{ij} \frac{\partial}{\partial v}, \frac{E_r}{v}$$

(i.e., to carry out the above integrals, one will need to generate a 2-D matrix of  $\frac{\partial}{\partial v}$ 's vs. these parameters for each flux surface)

This model is motivated by the more complete DKES calculations that indicate electrons are generally in the  $1/\Box$  regime:

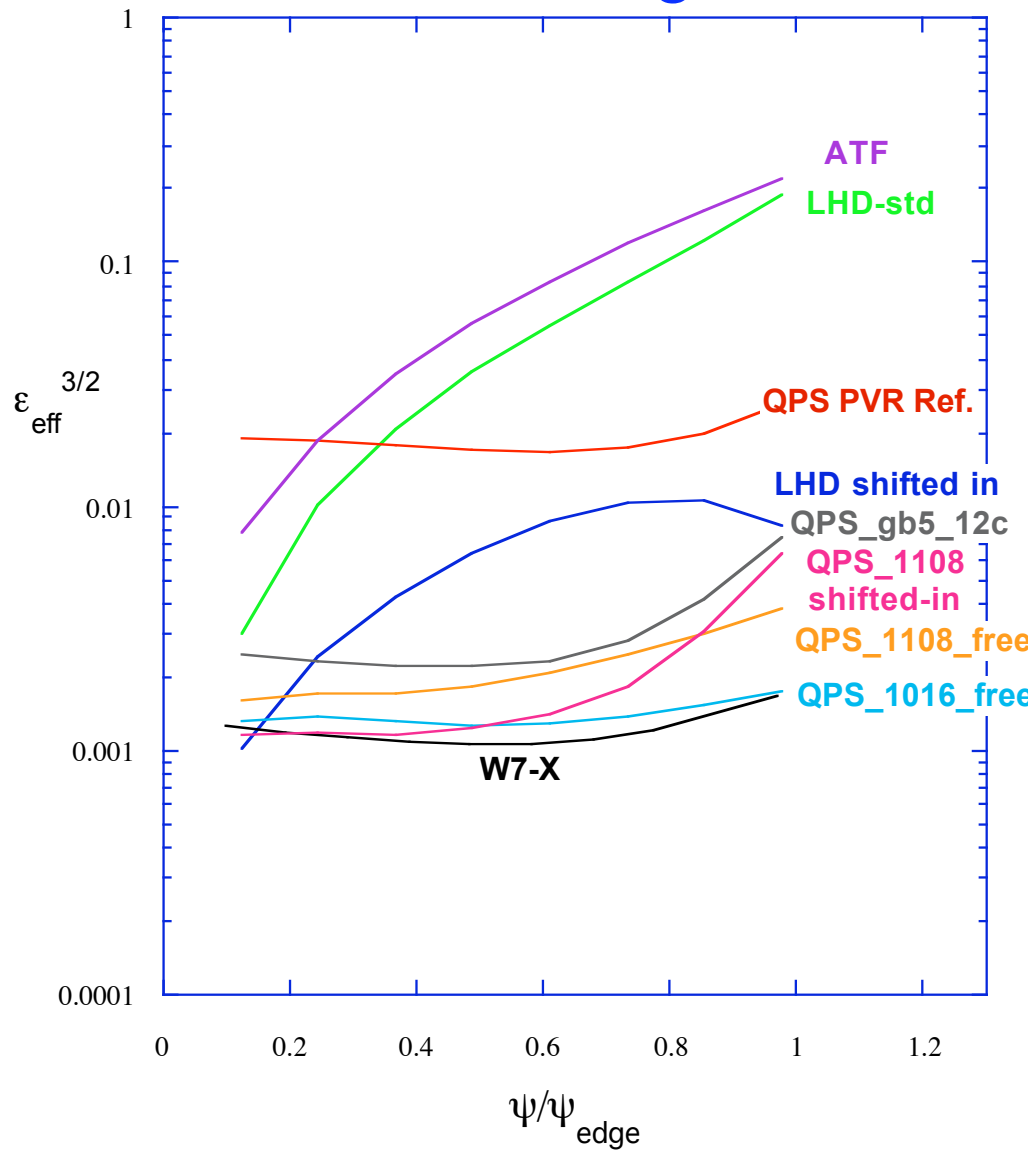


Typical DKES ambipolar calculations also show that overall transport level is generally set by lowering ion flux down to that of the electrons.

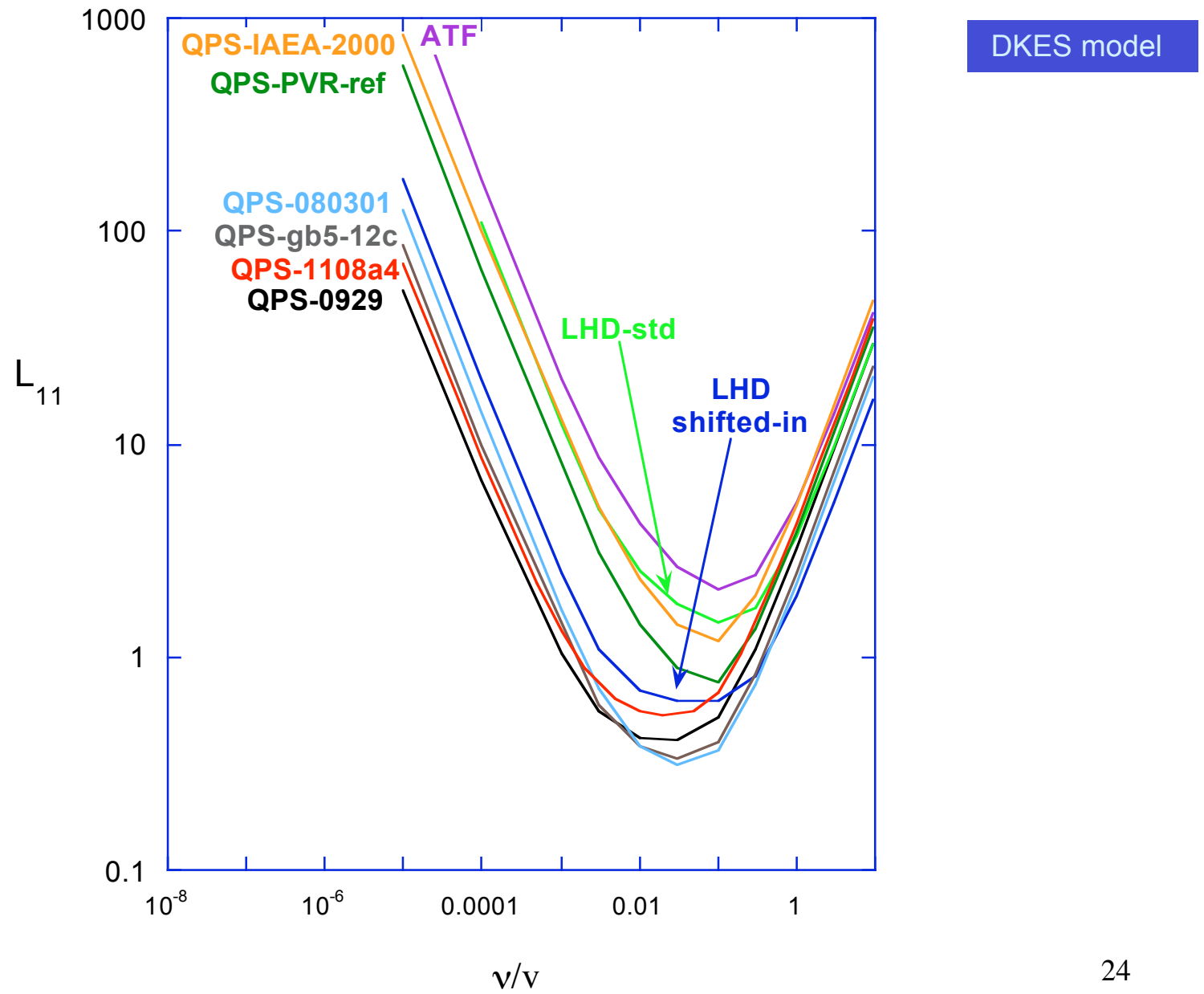


NEO code provides  $\bar{\Phi}_{\text{eff}}^{3/2} \sim D^{1/\beta}, \bar{\Phi}^{1/\beta}$ . Demonstrates effectiveness of NEO/DKES optimizations over a series of configurations

NEO  $\bar{\Phi}_{\text{eff}}$  code

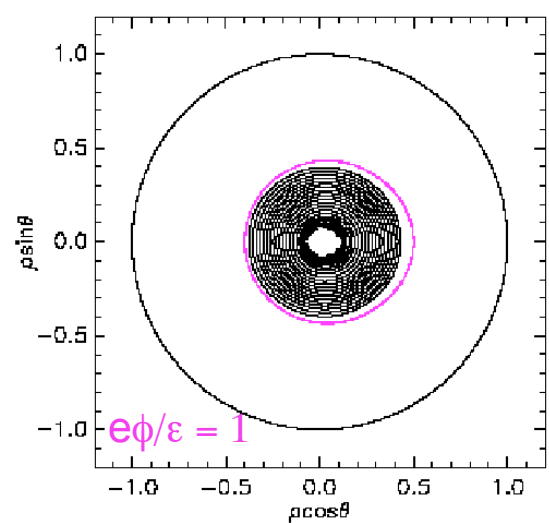
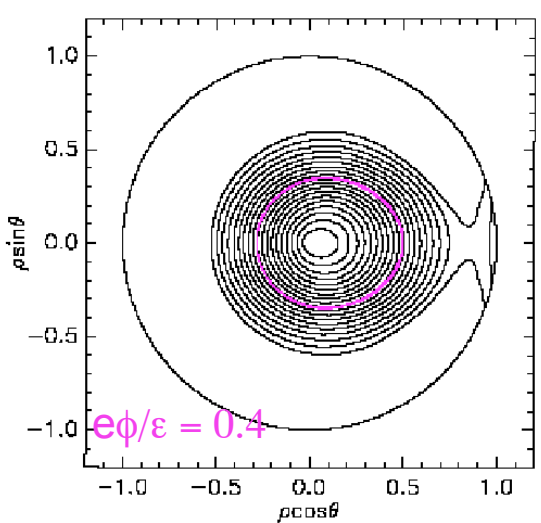
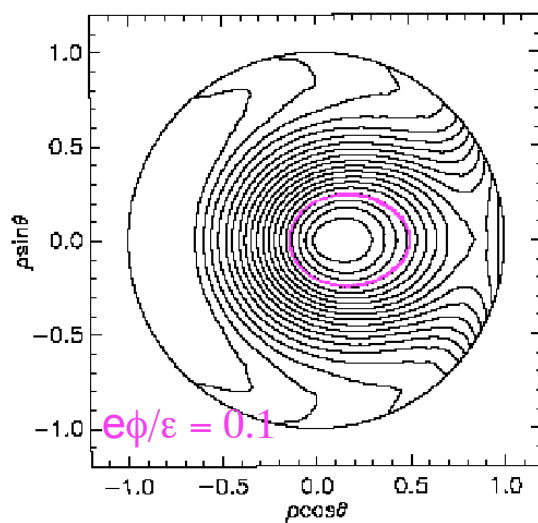
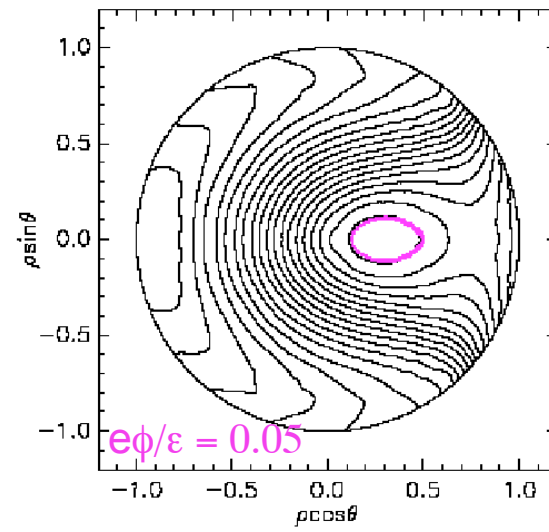
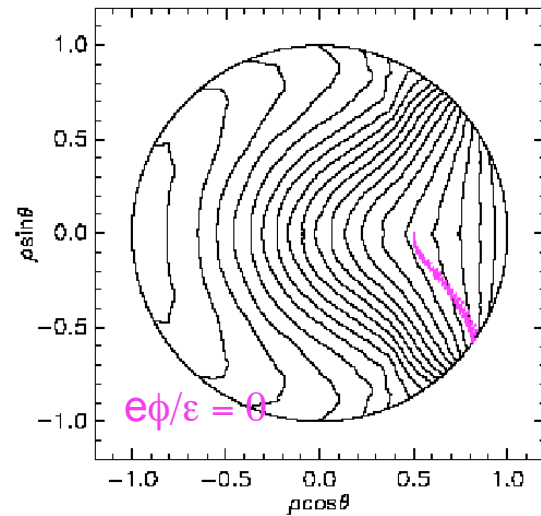
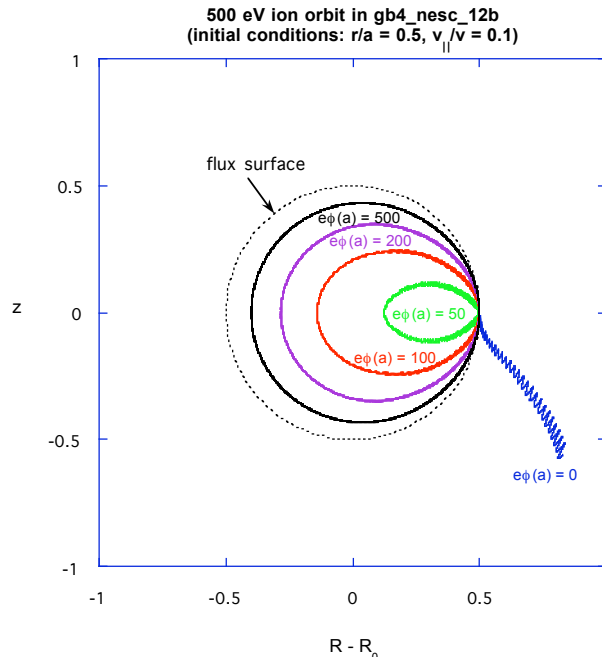


DKES  $L_{11}$  transport coefficient at  $E_r/v = 0.0001$  show similar trends at low collisionality among gb4/gb5 devices as NEO  $\bar{\ell}_{\text{eff}}^{3/2}$  coefficient

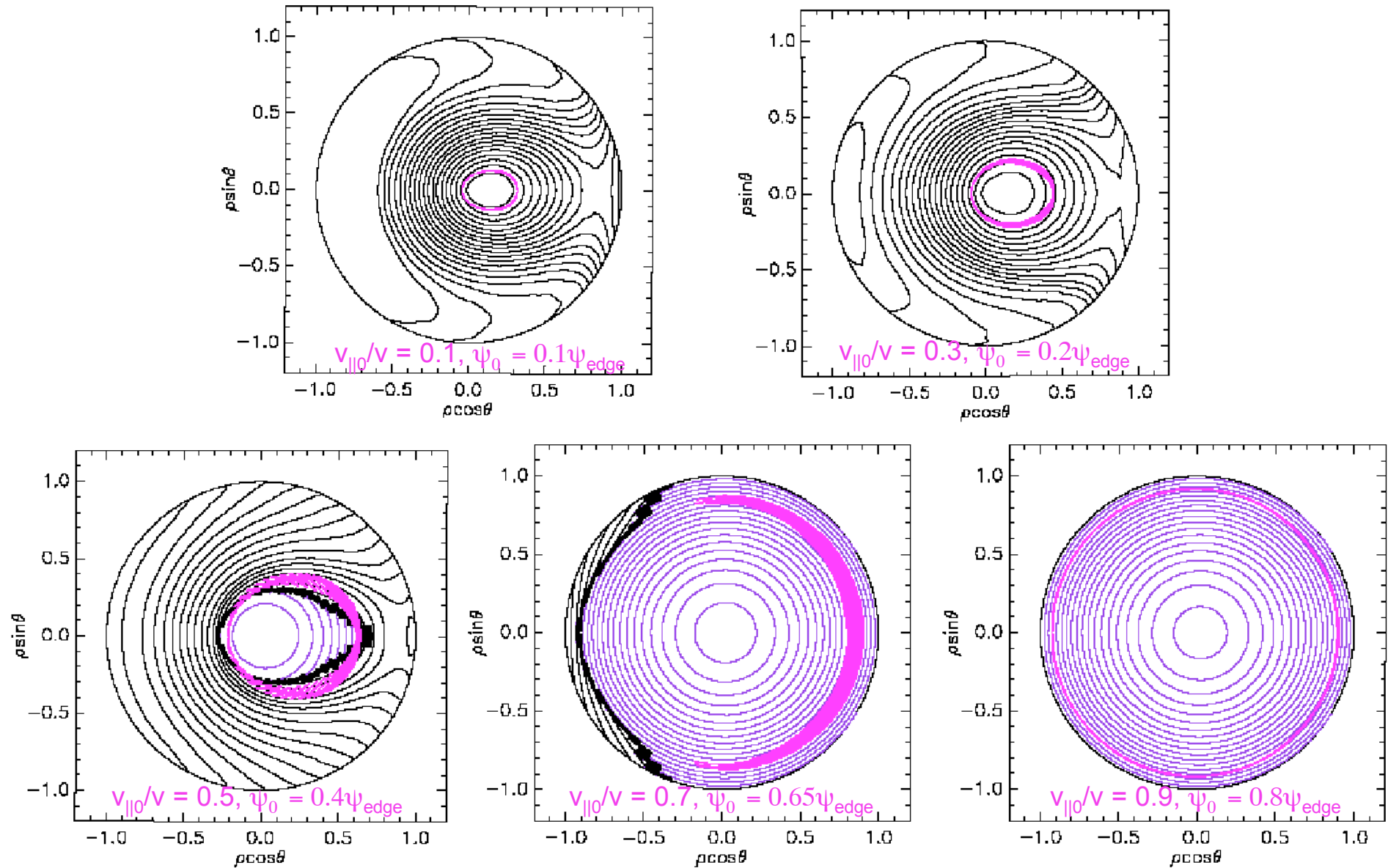


# ***QPS ORBITS AND MONTE CARLO SIMULATION***

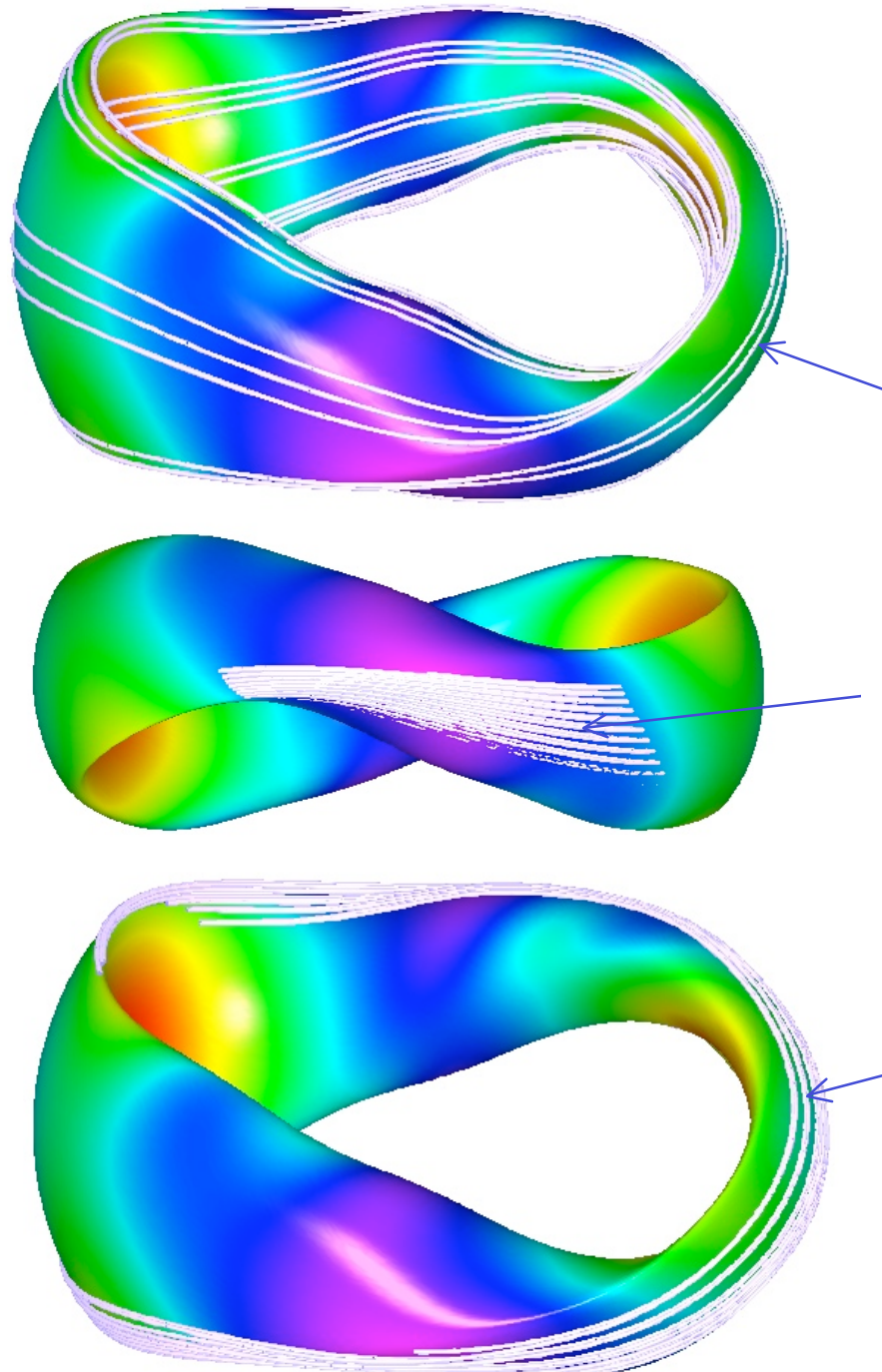
# Improvement of trapped 500 eV ion orbits with electric fields and alignment with $J^*$ contours



Alignment of  $v_{||0}/v = 0.1, 0.3, 0.5, 0.7, 0.9$  500 eV ion orbits with  $J^*$  contours  
 (black contours = locally trapped, purple contours = passing, magenta = orbit)



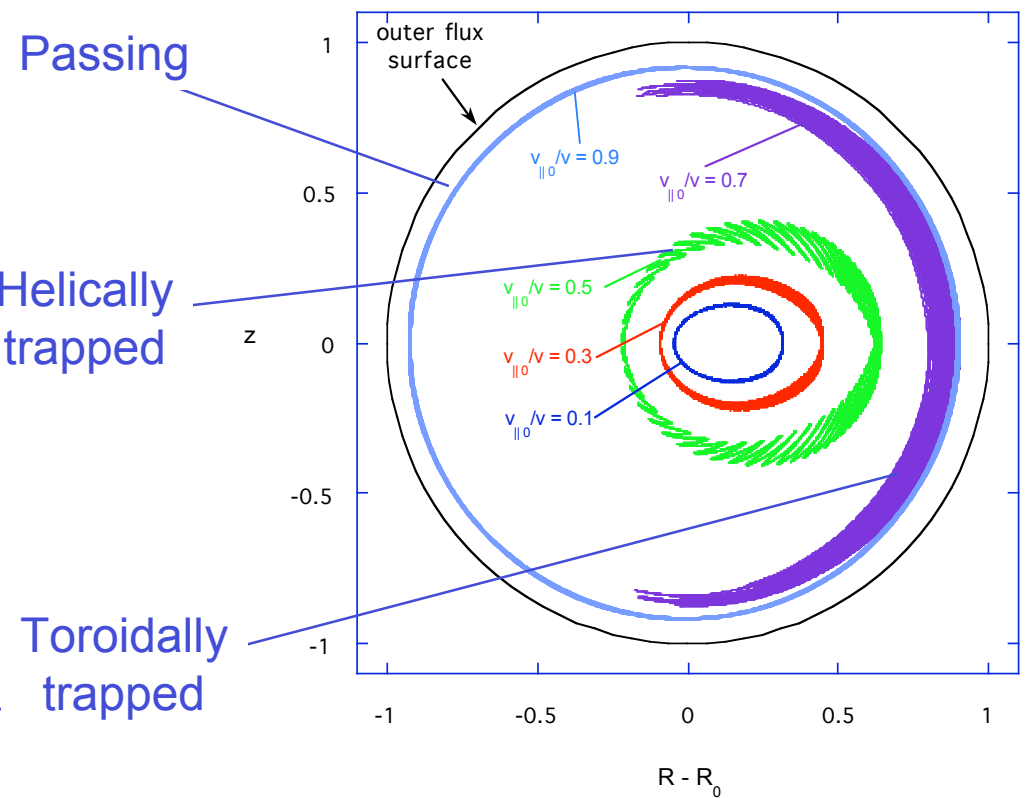
# QPS orbit topologies



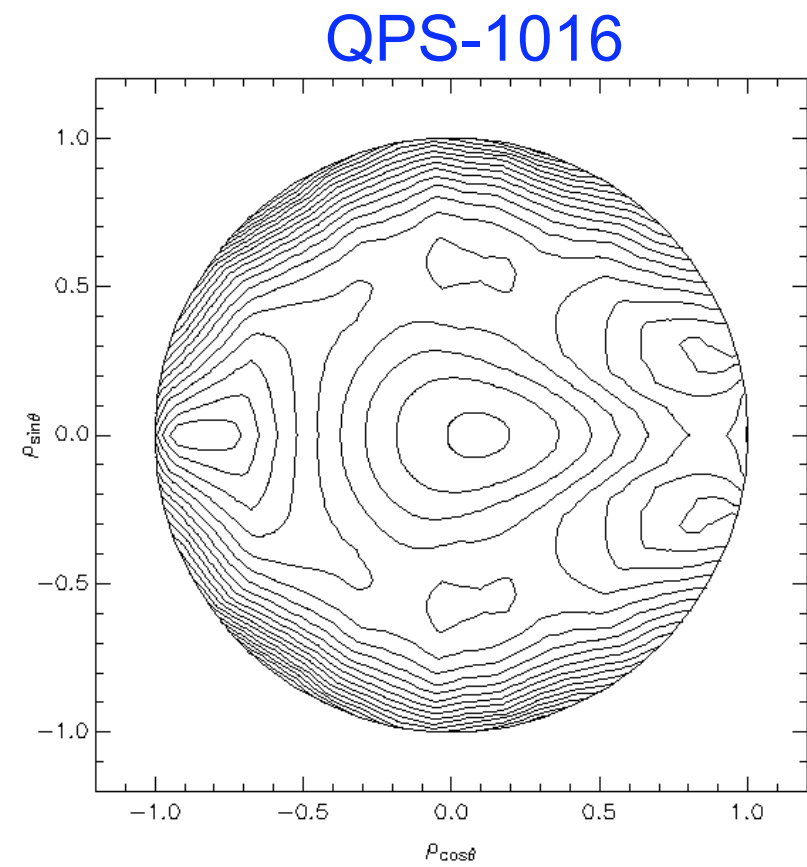
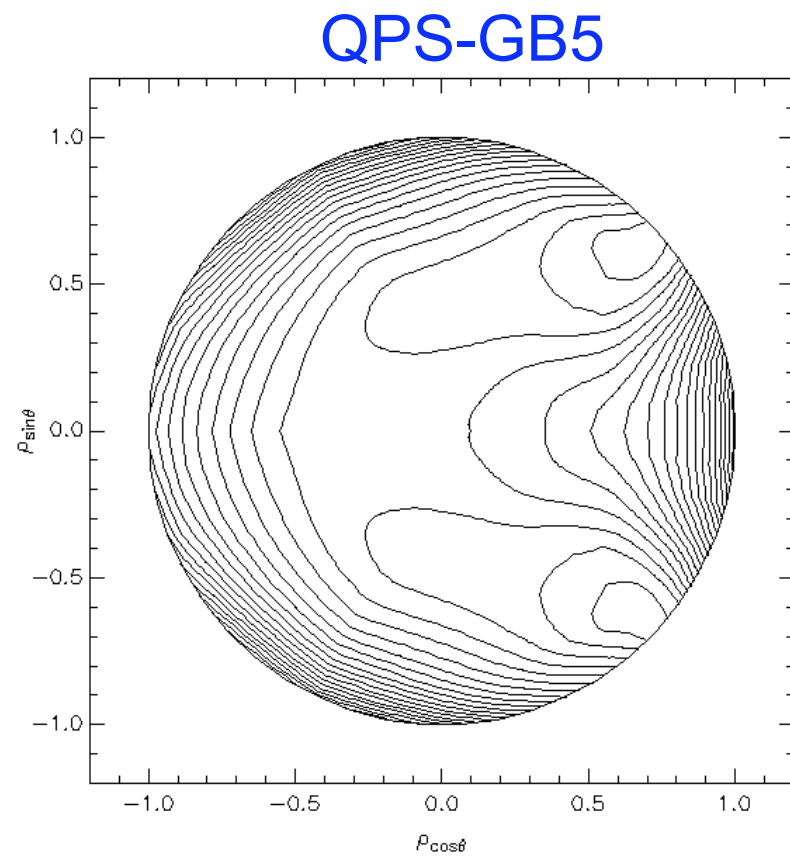
Passing

Helically trapped

Toroidally trapped



The recent QPS-1016 configuration improves the closure and centering of  $B_{\min}$  contours:

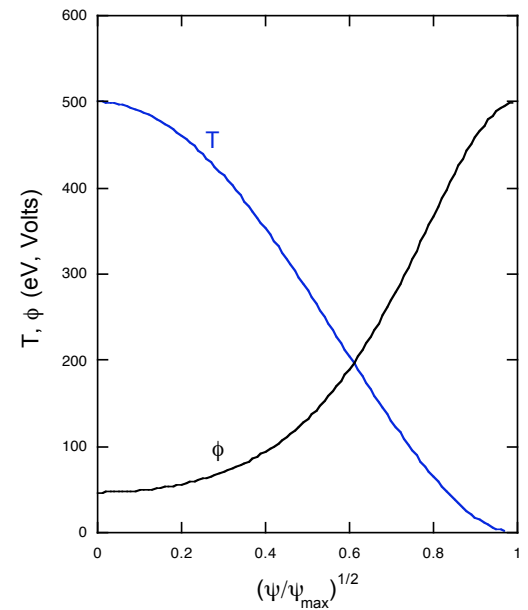
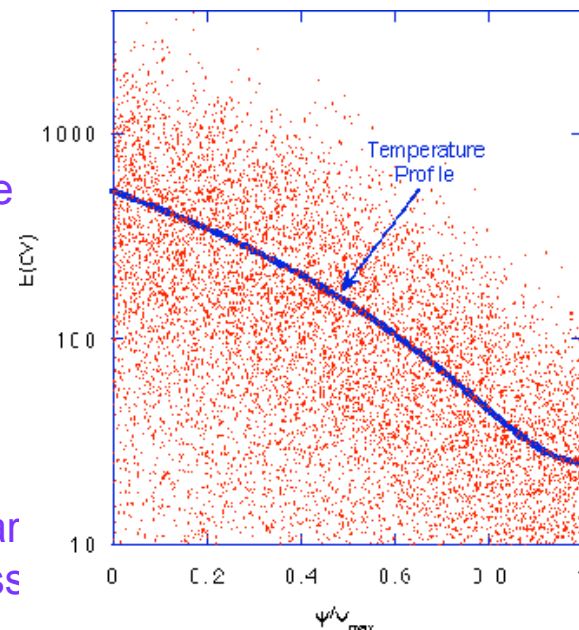


# Monte Carlo procedure for estimating global energy lifetimes (DELTA5D code)

DELTA5D Monte Carlo

- start with particles distributed over cross section using PDF's consistent with assumed profiles and local Maxwellians
- follow ensemble in time, replacing particles (consistent with initial PDF's) as they leave outer surface
- Record energies of escaping particles - use to calculate  $\bar{\tau}_E$
- Follow until approximate steady-state is achieved
- Vary potential (with fixed profile shape) to achieve global ambipolar balance of electron/ion particle loss rates

Typical initial Maxwellian particle loading for  $T = 500\text{eV}$   $(1 - \psi/\psi_{\max})^2$



## Power flows for global single species test particle simulations:

- To achieve steady state, in a reasonable simulation time, terms (1) and (2) need to be balanced:
- For  $E_r = 0$

$$\frac{dW_{test,ion}}{dt} = \int (Q_{ii} + Q_{ei}) d^3v \quad (+/-) \quad (1)$$

$$+ \int \vec{j} \cdot \vec{E} d^3v \quad (+/-) \quad (2)$$

$$+ \int \frac{dW_{surface\ loss}}{dt} dS \quad (-) \quad (3)$$

$$+ \int N_{replacement} [T(\square) + e\square] d^3v \quad (+/-) \quad (4)$$

$$\frac{dW_{test, electron}}{dt} = \text{Similar equations}$$

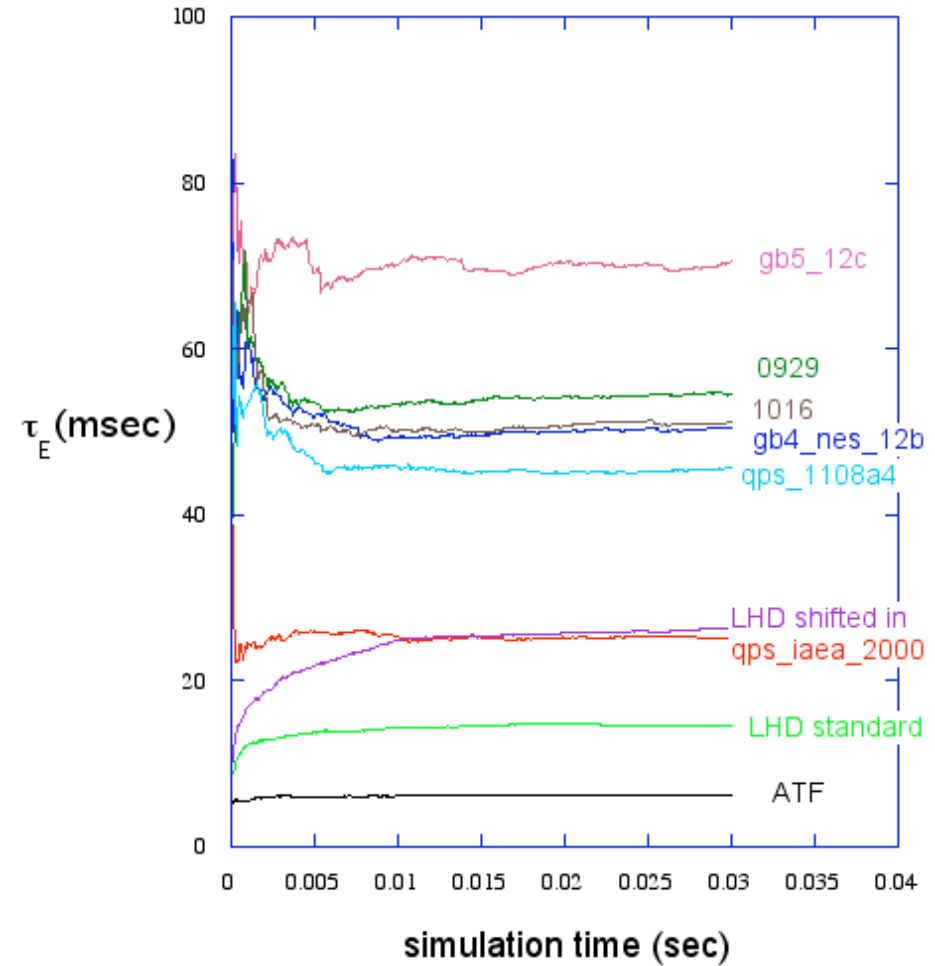
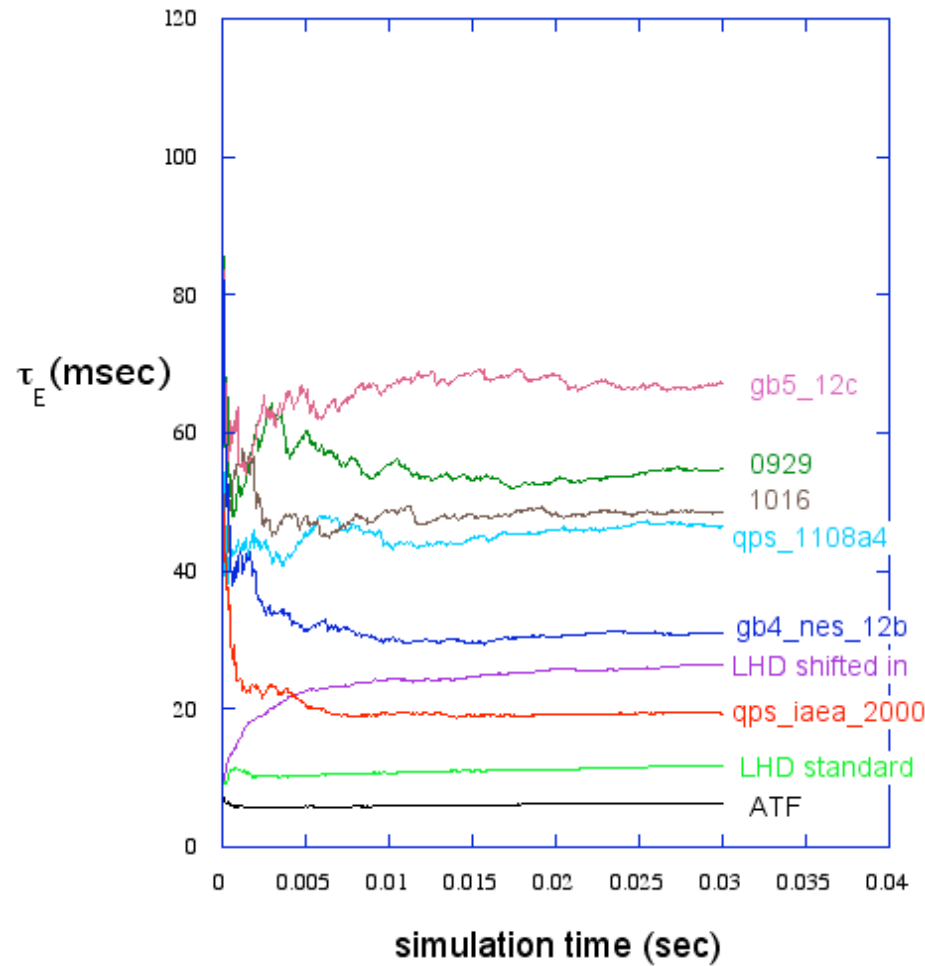
DELTA5D Monte Carlo

- For  $E_r \neq 0$ 
  - rely on  $Q_{ii} + Q_{ei}$  term (1) to redistribute energy loss/gain from term (2)
  - or can remove kinetic energy loss/gain (due to  $e\square$ ) each time step

# Comparison of Ion Monte Carlo lifetimes among different configurations (all scaled to constant $R_{\max}$ and $\langle B \rangle$ )

ECH regime:  $n(0) = 1.8 \times 10^{19} \text{ m}^{-3}$ ,  $T_e(0) = 1400 \text{ eV}$ ,  $T_i(0) = 150 \text{ eV}$

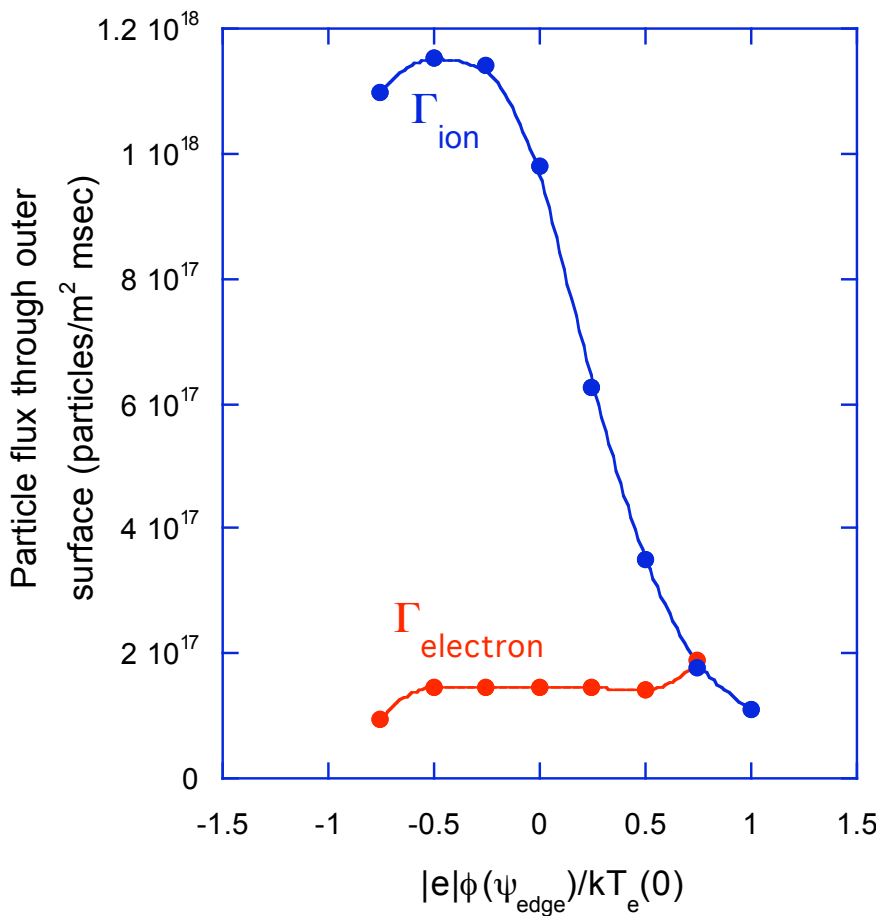
ICH regime:  $n(0) = 8.3 \times 10^{19} \text{ m}^{-3}$ ,  $T_e(0) = 500 \text{ eV}$ ,  $T_i(0) = 500 \text{ eV}$



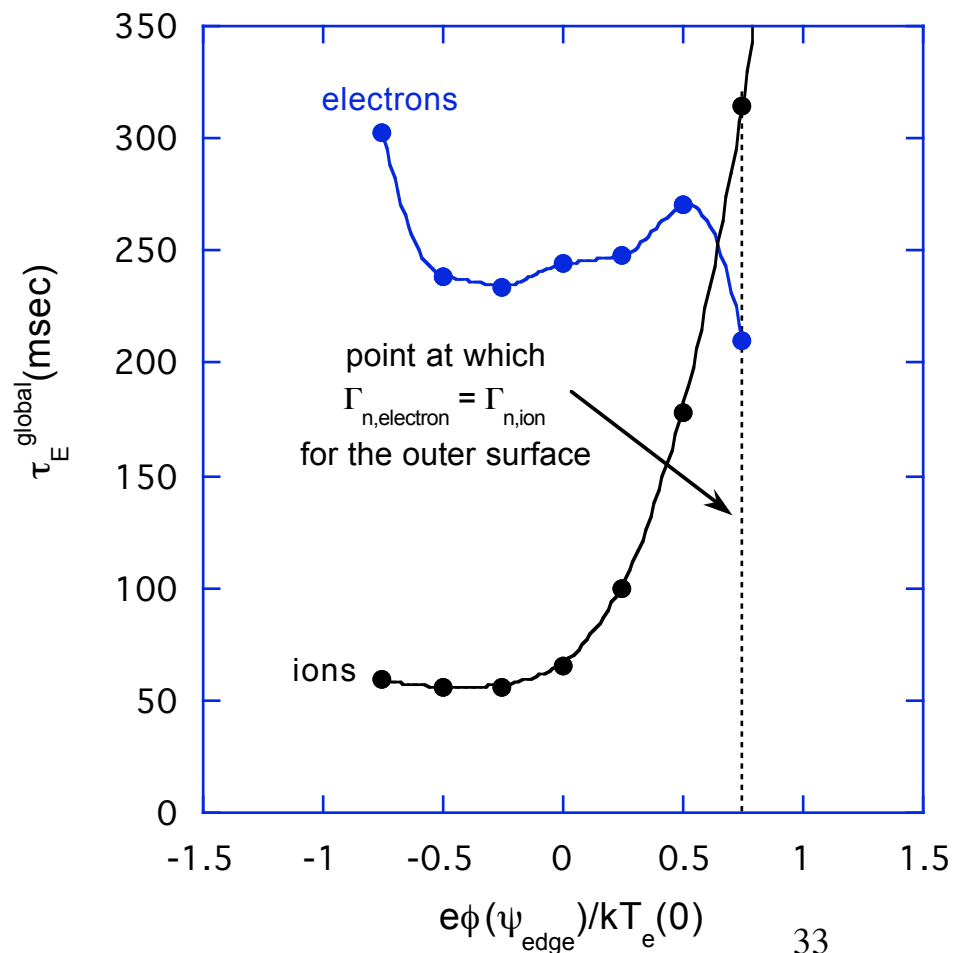
## Monte Carlo lifetimes for ICH heated gb4 configuration

$[n(0) = 8.3 \times 10^{19} \text{ m}^{-3}$ ,  $T_e(0) = 500 \text{ eV}$ ,  $T_i(0) = 500 \text{ eV}$ , flat density profile, parabolic<sup>\*\*2</sup> temperature profile]

Global ambipolarity condition  
[i.e., with  $\square(r)$  profile fixed]



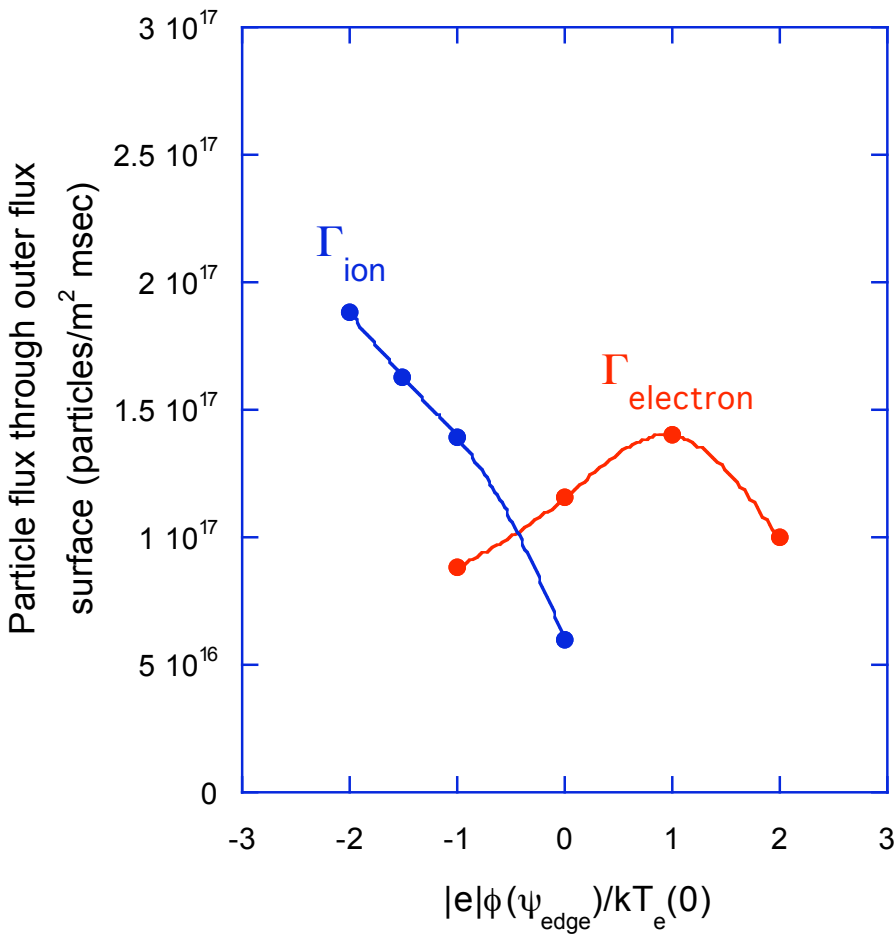
Global electron/ion energy lifetimes



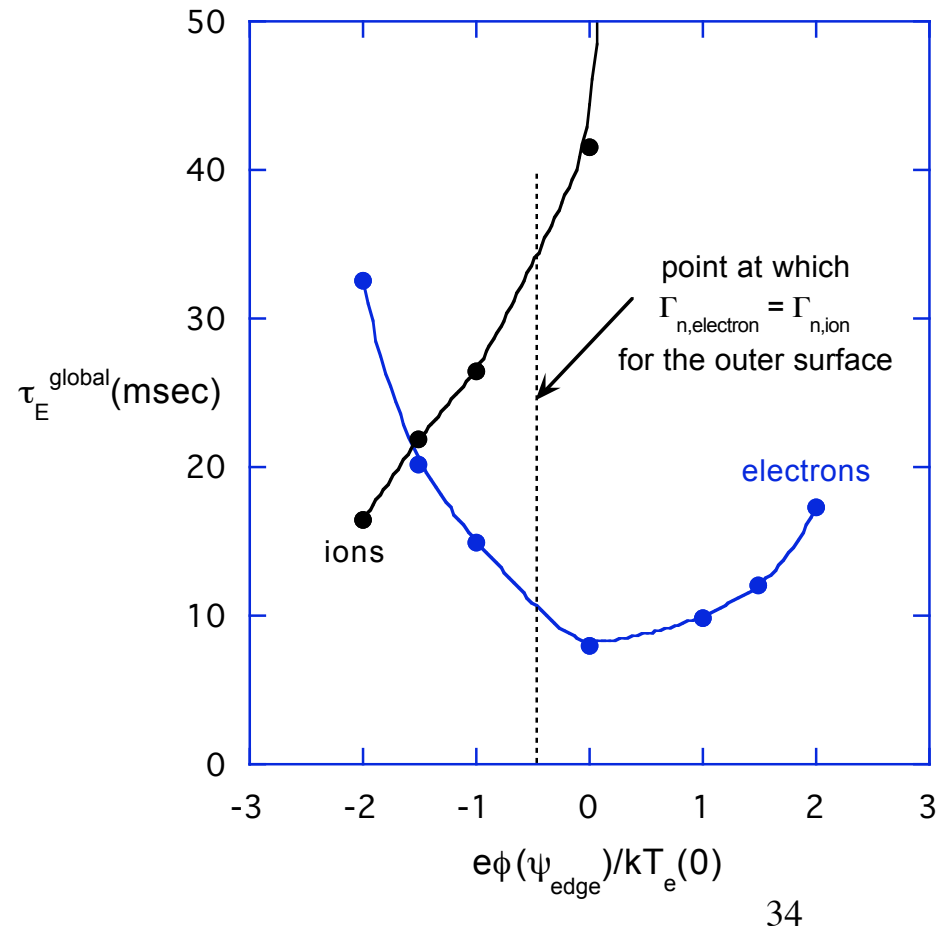
## Monte Carlo lifetimes for ECH heated gb4 configuration

[ $n(0) = 1.8 \times 10^{19} \text{ m}^{-3}$ ,  $T_e(0) = 1400 \text{ eV}$ ,  $T_i(0) = 150 \text{ eV}$ , flat density profile, parabolic\*\*2 temperature profile]

Global ambipolarity condition  
[i.e., with  $\mathbb{Q}(r)$  profile fixed]



Global electron/ion energy lifetimes

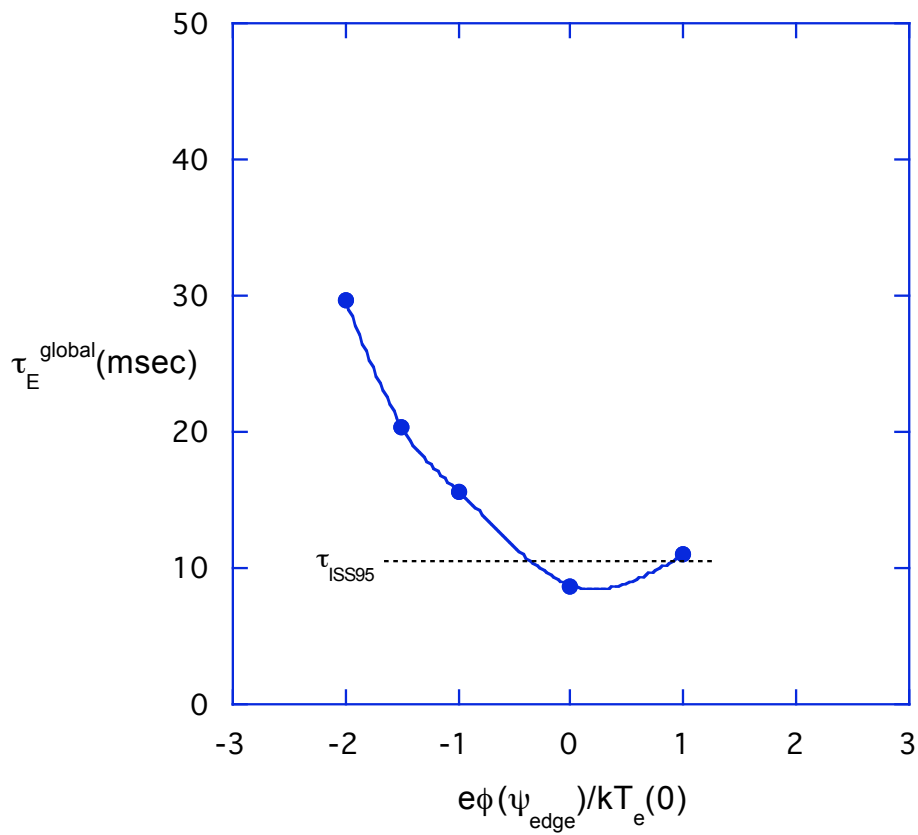


Comparison of ECH/ICH global lifetimes with ISS95 scaling law for GB4 configuration

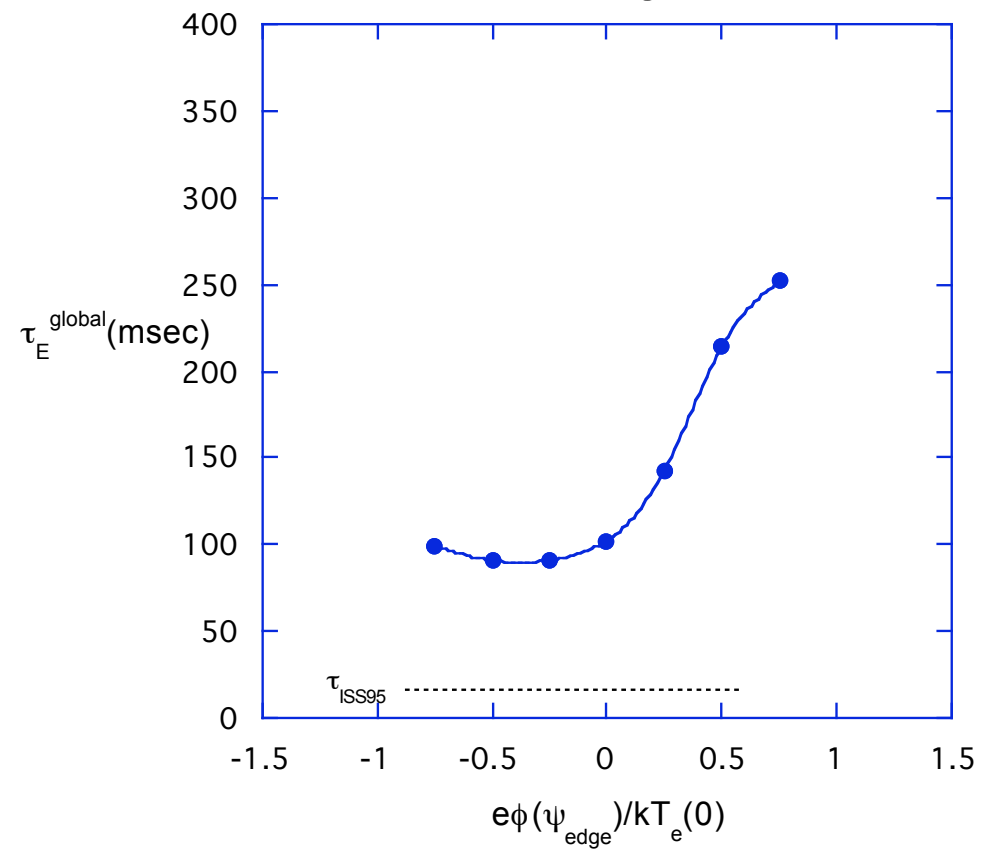
$\square_{gl}^{MC}$  = global lifetime, taking into account electron and ion loss channels:

$$\square_{gl}^{MC} = \frac{(T_e + T_i) \square_e \square_i}{T_e \square_i + T_i \square_e}$$

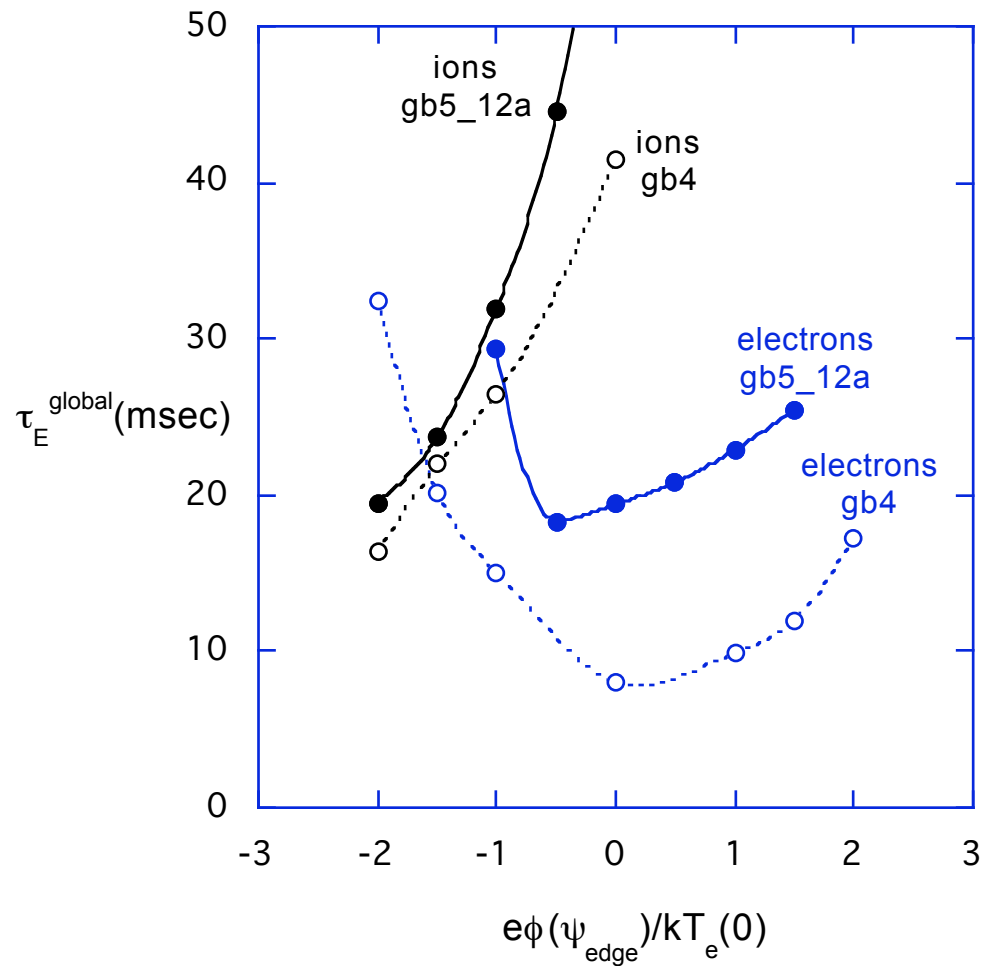
ECH heated gb4 case



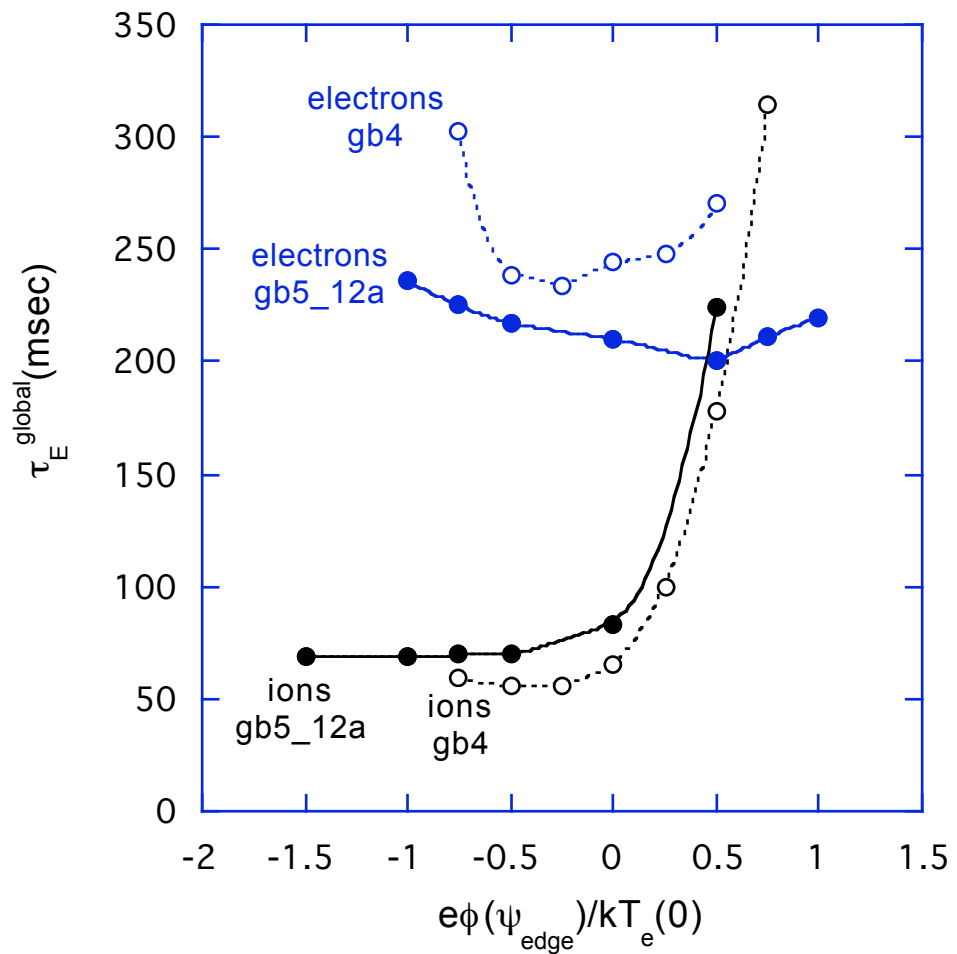
ICH heated gb4 case



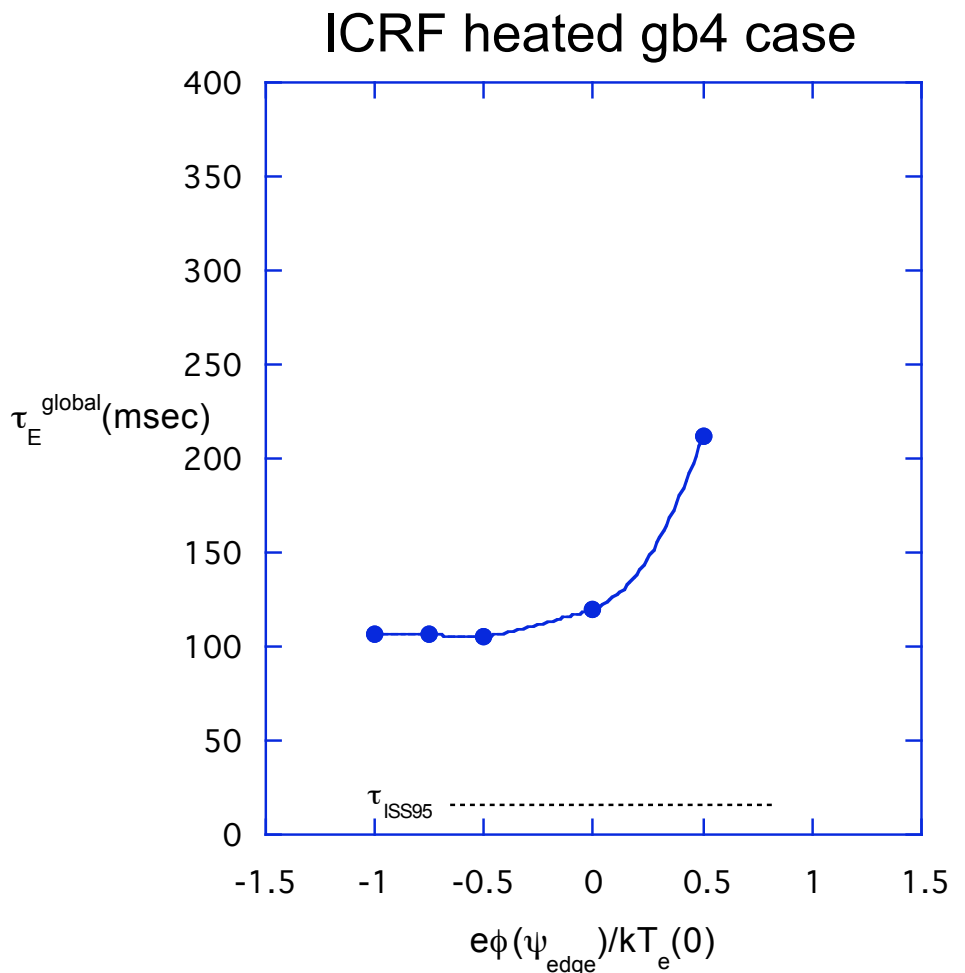
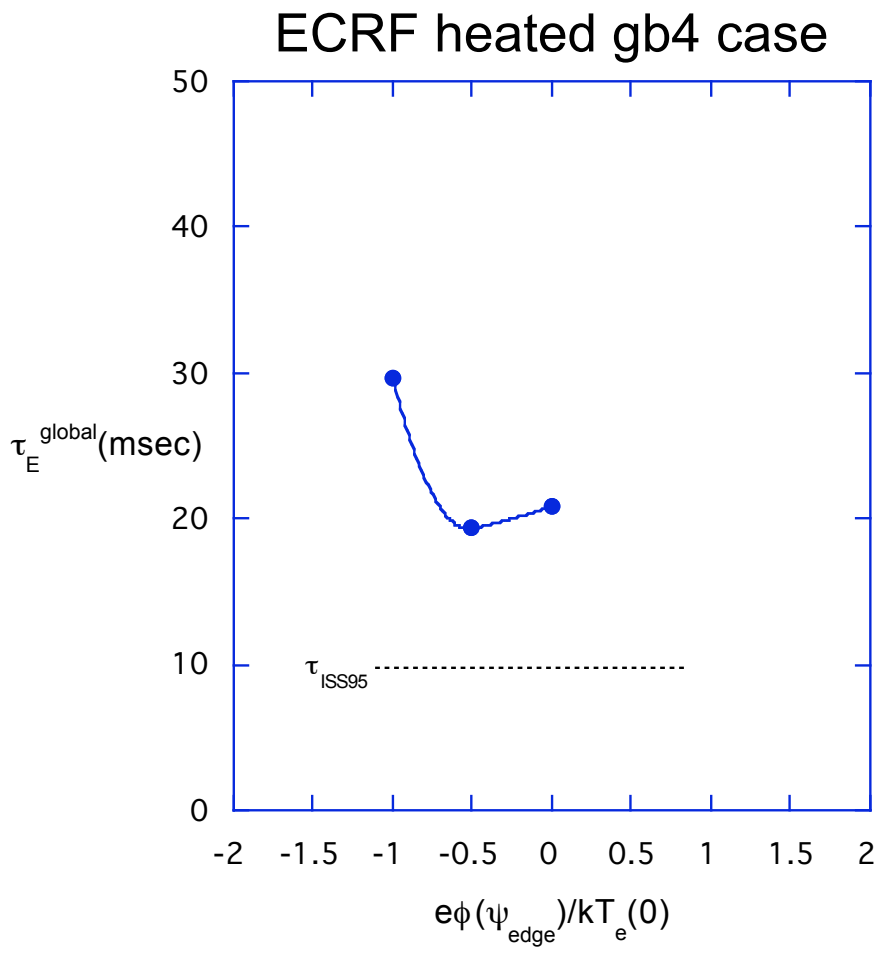
## Comparison of gb4 and gb5 global lifetimes for ECH parameters



## Comparison of gb4 and gb5 global lifetimes for ICH parameters

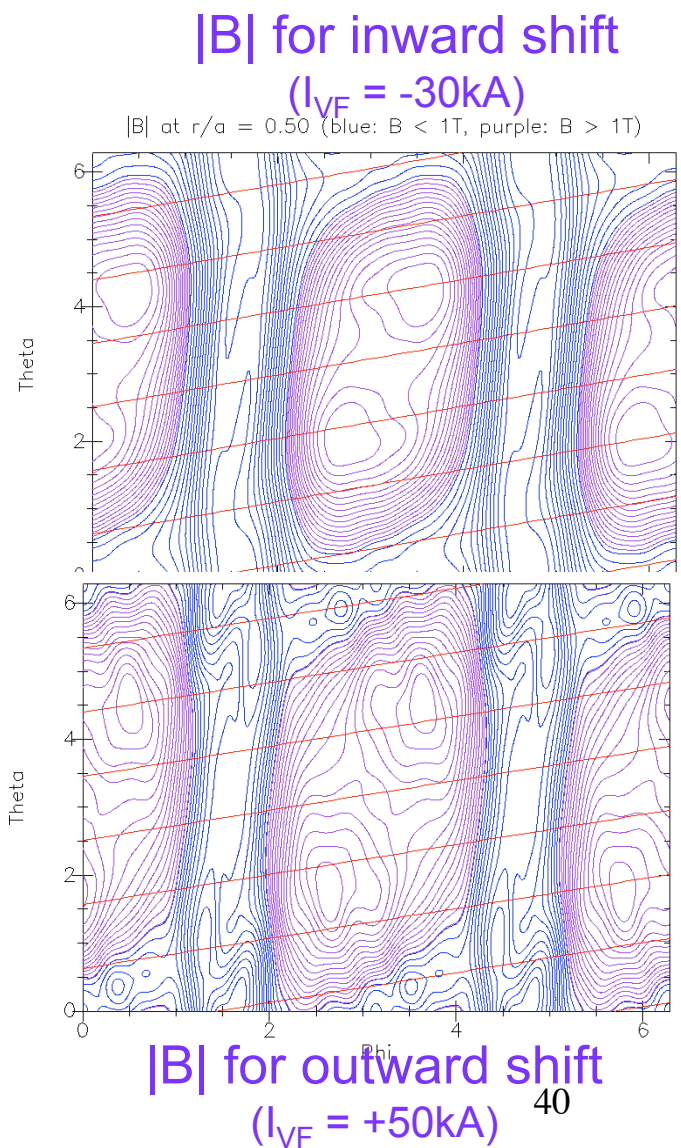
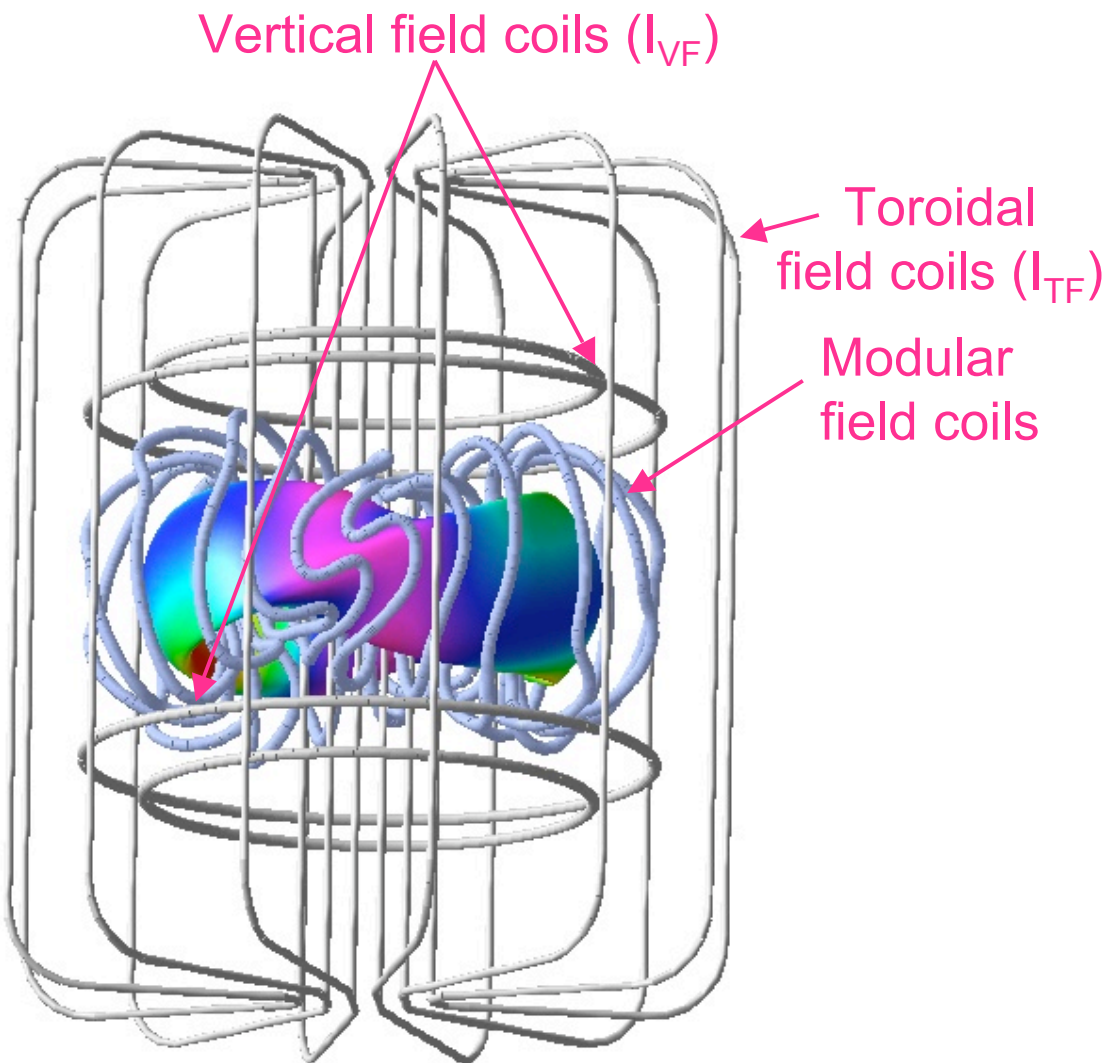


Comparison of ECH/ICH global lifetimes with ISS95 scaling law for  
GB5\_12A configuration

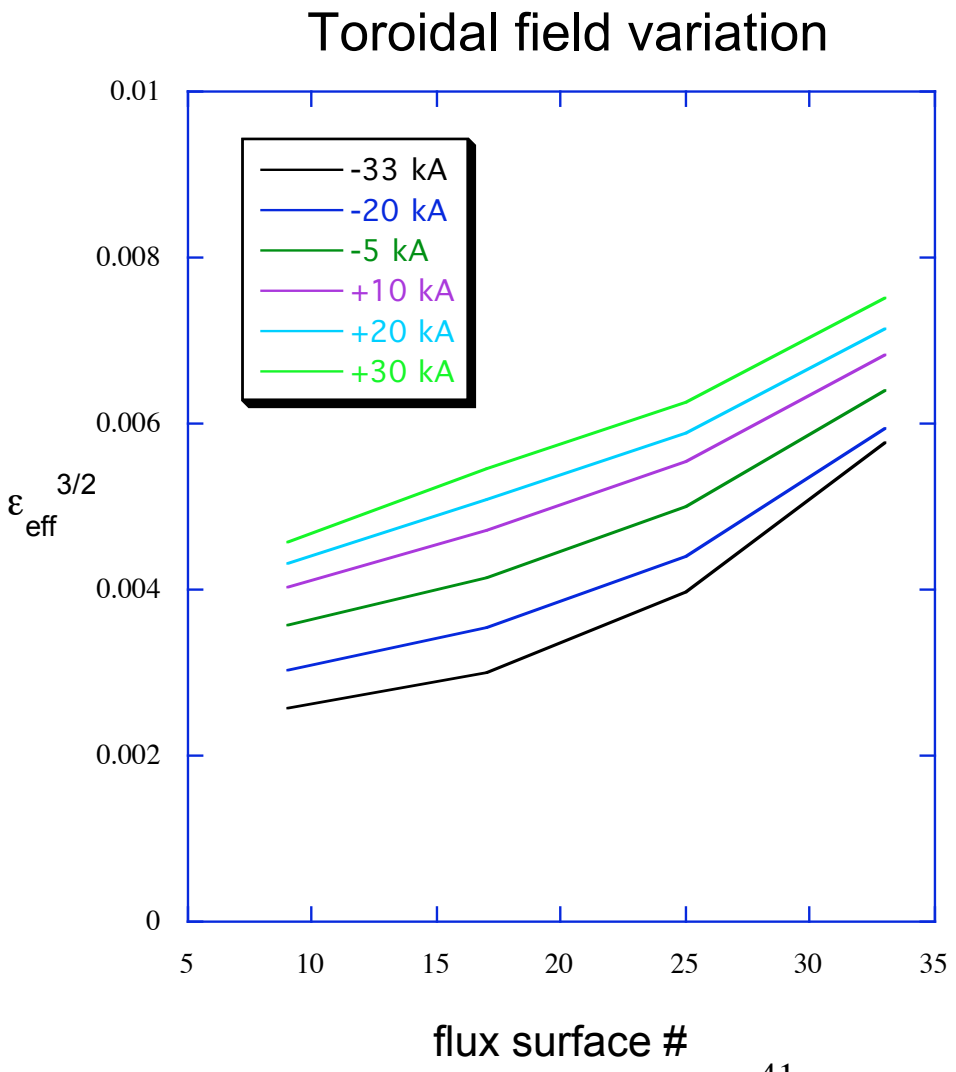
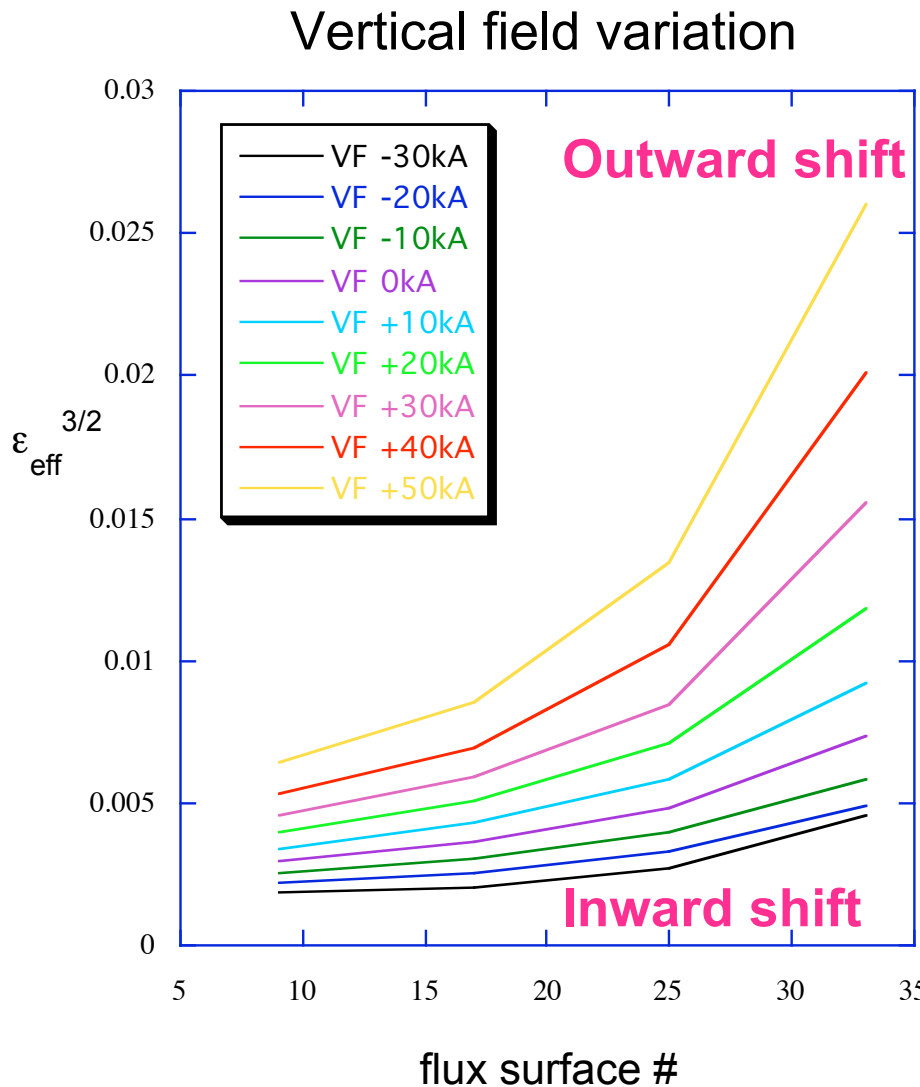


# ***QPS FLEXIBILITY STUDIES***

Flexibility is provided in QPS by 3 main coilsets.  
By changing these coil currents, different configurations are possible.



Transport properties can be influenced either by varying the vertical or toroidal fields.



## Conclusions

- QPS should be able to reach the plasma performance needed for its mission
- ISS95 scaling + ripple transport (0-D and 1-D) predict good performance
- Monte Carlo calculations of neoclassical component show that it is not a limiting feature
- The current configuration offers flexibility through the vertical, toroidal and modular coil currents
- A spectrum of transport analysis tools has been developed which - form a good basis for supporting a future experiment